6-20-2016

Synthesis of Dual Rod-coil Brush Polymers and Their Solution Properties

xixian ye
xixian.ye@uconn.edu

Synthesis of Dual Rod-coil Brush Polymers and Their Solution Properties

Xixian Ye

B.S., Fudan University, Department of Macromolecular Science and Engineering,

2010

A Thesis

Submitted in Partial Fulfillment of the

Requirements for the Degree of

Master of Science

University of Connecticut

2016

APPROVAL PAGE

Masters of Science Thesis

Synthesis of Dual Rod-coil Brush Polymers and Their Solution Properties

Presented by

Xixian Ye, B.S.

Major Advisor: Yao Lin, Ph.D

Major co-Advisor: Rajeswari Kasi, Ph,D

Associate Advisor: Jie He, Ph.D

University of Connecticut

2016

ACKNOWLEDGEMENT

I would like to express my gratitude to my parents and friends overseas who supported me to finish my degree. They were on the other side of the ocean, accompany me working in the lab on many sleepless nights.

I would like to especially thank for the kindness of my advisors Dr. Lin and Dr. Kasi. They are not only my advisors for the project, providing suggestions on my research but also helped me with a lot of troubles in daily life. I am lucky to be their student. I would also like to thank my committee advisor Dr. Jie He who gave me valuable suggestions on my research.

Finally, I would like to thank my group members for supporting my research and Mrs. Charlene Fuller, I enjoyed talking and walking with her during the lunch hour. And I also want to thank the other faculty and staff in Chemistry Department and IMS who helped me and advised me on every aspects of my life in Uconn.

Table of Contents

ABSTRACT

Dual rod-coil brush copolymer [Polynorbornene-graft-Poly(3-hexylthiophene)]-block-[polynorbornene-graft-Poly(ethylene oxide)] [(PNB-g-P3HT)-b-(PNB-g-PEO)] (P3HT-PEO) was synthesized via Grignard Method, click chemistry and Ring Opening Metathesis Polymerization to observe nanostructures. However, due to the unknown reason, early degradation was occurred disabling formation of architectures in the melts. Unique hollow nanoband was observed in DCM and Methanol solution, which may result from a coeffect of π-conjugated aggregation and microphase separation. And a clear transition between J- and H- aggregation occurs when changing solution mixtures in dual brush copolymer system.

Chapter One

Introduction

Copolymers contain different blocks can self-assemble into ordered architectures. The driving force of those structures comes from microphase separation in the bulk and solvophilic/solventphobic forces in the solution. When there are more than one crystallizable block, crystallization can also contribute to the process both in the bulk and in solutions. Linear copolymer polystyrene-b-poly(ethylene oxide) (PS-b-PEO) for example, structures such as tubular, vesicle, lamella with protruding rods and rods were observed in solutions[1,2] and lamellar structures in melts[3]; more melt structures such as spherical, hexagonally packed cylinders, bicontinuous and perforated layers can be observed by controlling volume fractions and symmetry of blocks of polystyrene-b-polyisoprene (PS-b-PI)[4]. Most of relative studies were based on coil-coil copolymers, presenting random walk and flexible conformations (Figure 1.1).

	Chemical composition	Architecture	
melts	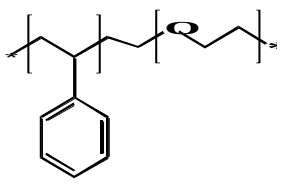	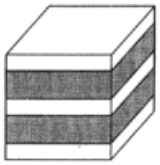 Lamellae	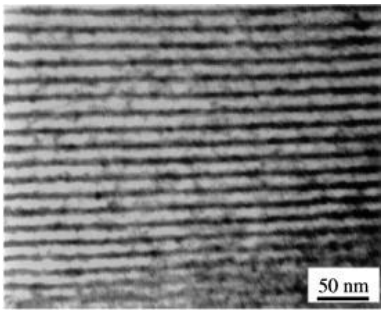

<table>
<tr><td rowspan="2"></td><td rowspan="2"> 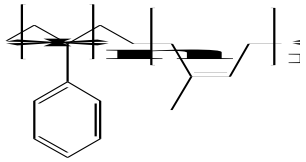 </td><td> 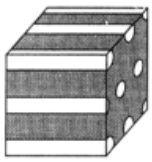
Cylinders</td><td> 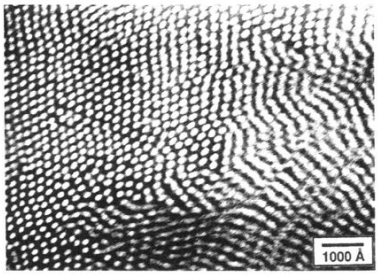 </td></tr>
<tr><td> 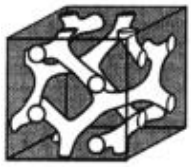
Bicontinuous</td><td> 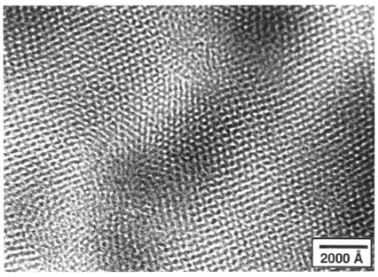 </td></tr>
<tr><td></td><td></td><td> 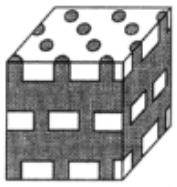
Perforated
Layers</td><td> 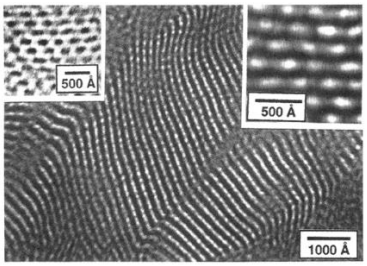 </td></tr>
<tr><td>solution</td><td> 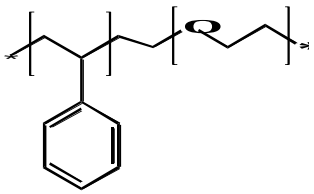 </td><td colspan="2"> 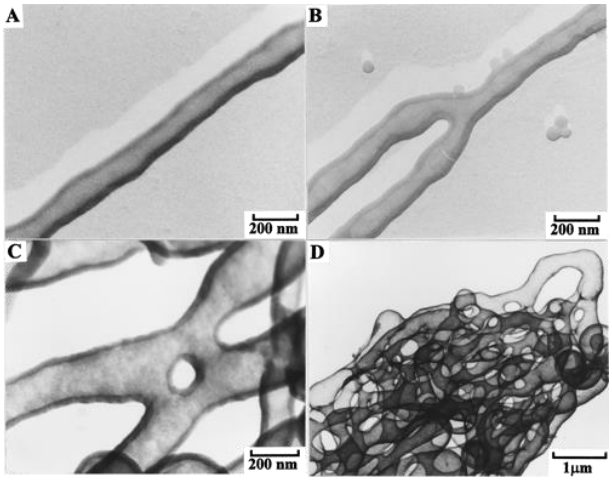
Tubular</td></tr>
</table>

		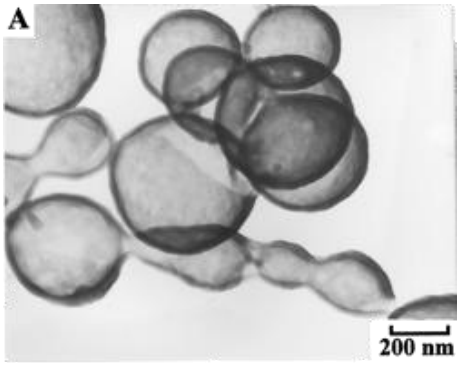 Vesicle
		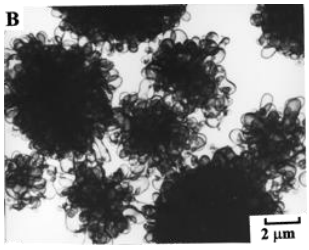 micelle
		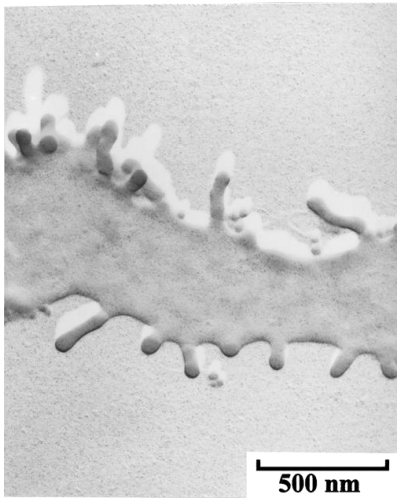 Lamella

		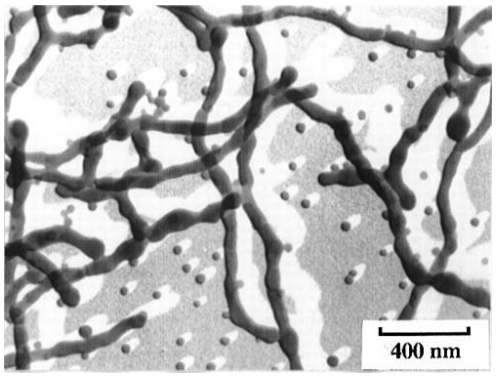 Rod

Figure 1.1: phase behaviors of linear coil-coil[3,4] polymer in melts and solutions[1,2]

It is also known that nanostructures of copolymers are related to polymer topology, for example, dual coil-coil brush polymer containing two types of side chains, presenting lamellar[5], cylinders[6] and sphere[7] were observed in the melts; and micelle, flower-like and dumbbell-like[8, 9,10] structures were observed in the solution. (Figure 1.2)

	Chemical Composition	Architecture

melt	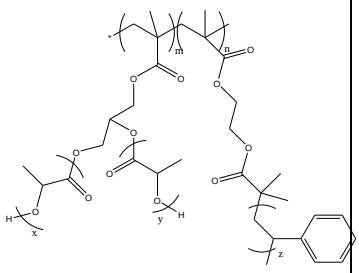	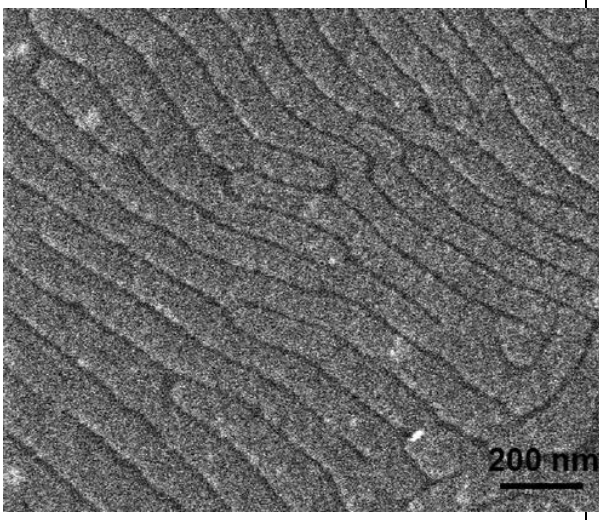 lamellar
	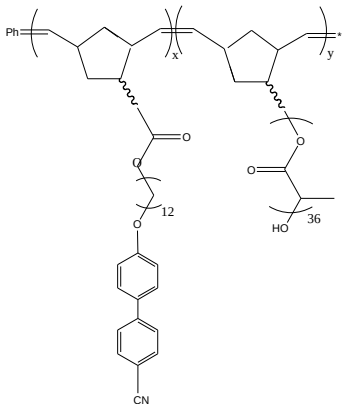	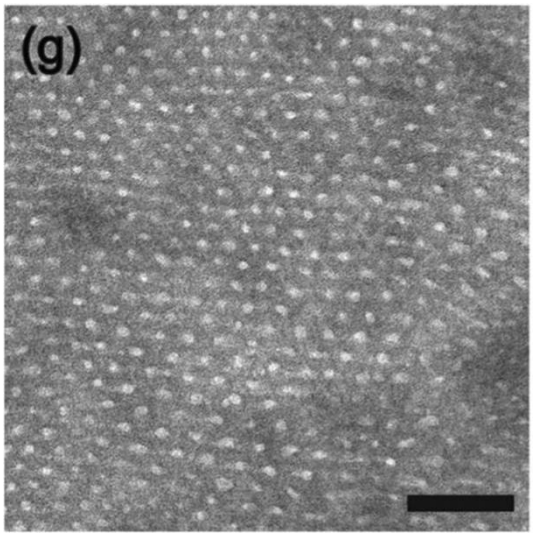 cylinder

	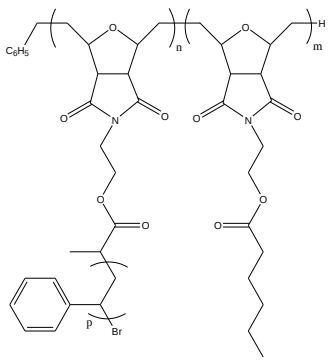	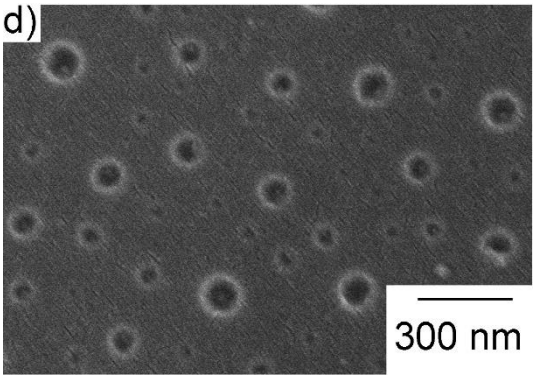 sphere
solution	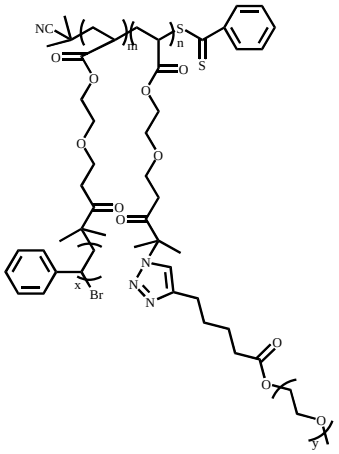	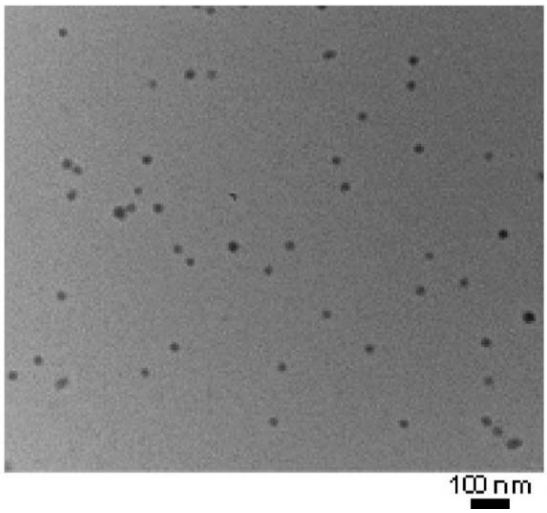 micelle

	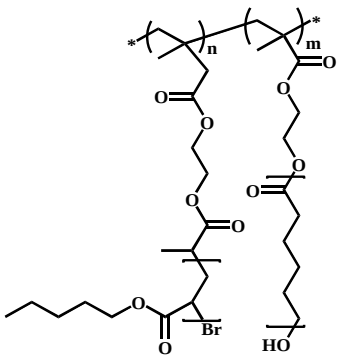	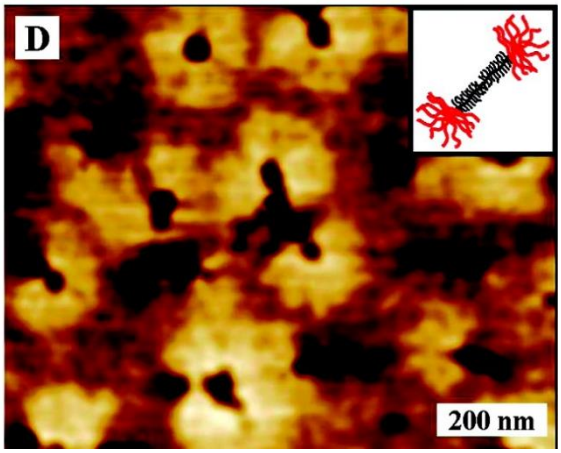 Dumbbell-like
	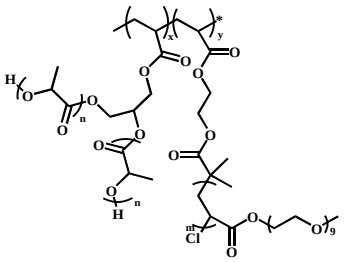	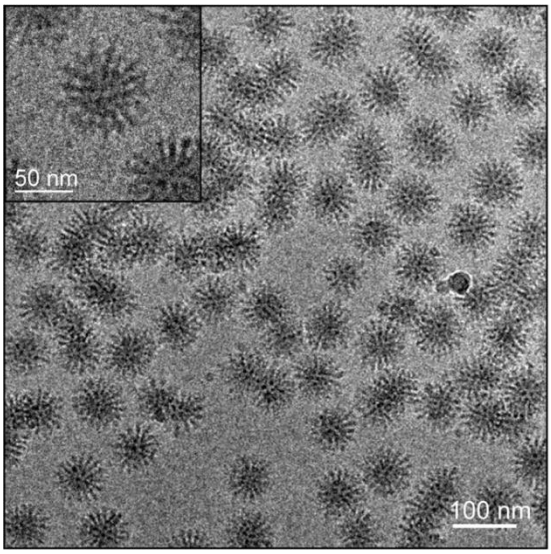 Flower-like

		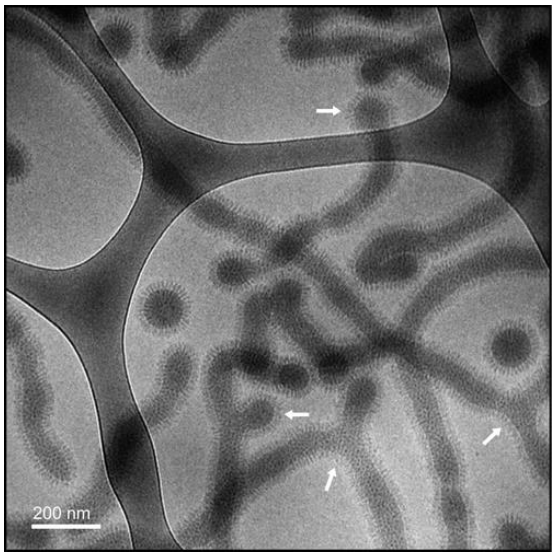 Y-junction

Figure 1.2: nanostructures formed from dual coil-coil brush copolymers[5-10]

On the contrary, when polymer contains π -conjugation, helical secondary structures (polypeptide) or aromatic groups along the backbone, it will form extended and rigid polymer chains (Figure 1.2). Those polymers are called rod polymers and rod-coil copolymers are wide-explored due to potential applications in organic electronics[11-13] , biotechnology[14, 15] and high performance composites[16, 17].

Their self-assembled architectures are different compared with coil-coil copolymers because of the following reasons: 1) the inflexibility nature of rod blocks, this topology leads to a different conformational entropy with coil blocks, disabling its accommodation packing by stretching and gaining conformational entropy; 2) anisotropic tendency of rods provides potential for liquid crystal ordering while

additional interactions may increase complexity of the system; and 3) rod polymer has characteristic size linearly corresponds to the degree of polymerization (N) at θ-condition while coil polymers scales as $N^{1/2}$, showing different scaling behaviors on the molecular level. Similar structures from coil-coil copolymers can also be observed from rod-coil copolymers while some unique structures like helices[18,19], ribbons[20], rings[21,22,23], tetragonally perforated lamellae (EPL)[24] , zigzag[25,26] and tubules[27,28] were observed.

Conjugated polymers are wide explored for the rapid needs of light and cheap semiconducting materials in solar cells[11], biosensors[12b,29] and field effect transistors[12a,13] in recent years. Their π -conjugations rigidify the backbone and at the same time also introduce conductivities along the chains. Nanostructures of conjugated polymers are proved to correlate with stacking and charge transfer defects[30,31], thus impacting physical properties and material performance[32,33,34,35,36]. Due to low processibility and physical performance, conjugated-coil copolymers are one of the methods that can overcome the shortage of homo-conjugated polymers.

Among various of conjugated polymers, polythiophene (PT) is an ideal starting material in the copolymers as its derivatives have good solubility, chemical stability and optoelectronic properties[30,34,37]. Among those synthesized and characterized PT-based copolymers, most of them are reported as linear polymers, e.g. poly(3-hexylthiophene)-b-poly(phenyl isocyanide) (P3HT-b-PPI)[36], poly(3-hexylthiophene)-b-poly(ethylene oxide) (P3HT-b-PEO)[38,39,40,41], poly(3-hexylthiophene)-b-polystyrene

(P3HT-b-PS)[42,43] and poly(3-hexylthiophene)-b-poly(lactide) (P3HT-b-PLA)[44]. Insulating coil polymers are introduced to improve solubility, flexibility, processiblity and manipulating nanostructures, as a result, well controlled supermolecular architectures of those block copolymers can be determined by block length, polydispersity index (PDI), volume fraction, chain flexibility etc. Vesicle, fiber, ribbons are formed under different solution and solvent mixtures[36,41,45,46]; micelle, lamellar and hexagonally packed microstructures are observed in the melting state[47, 48, 49] (Figure 1.3).

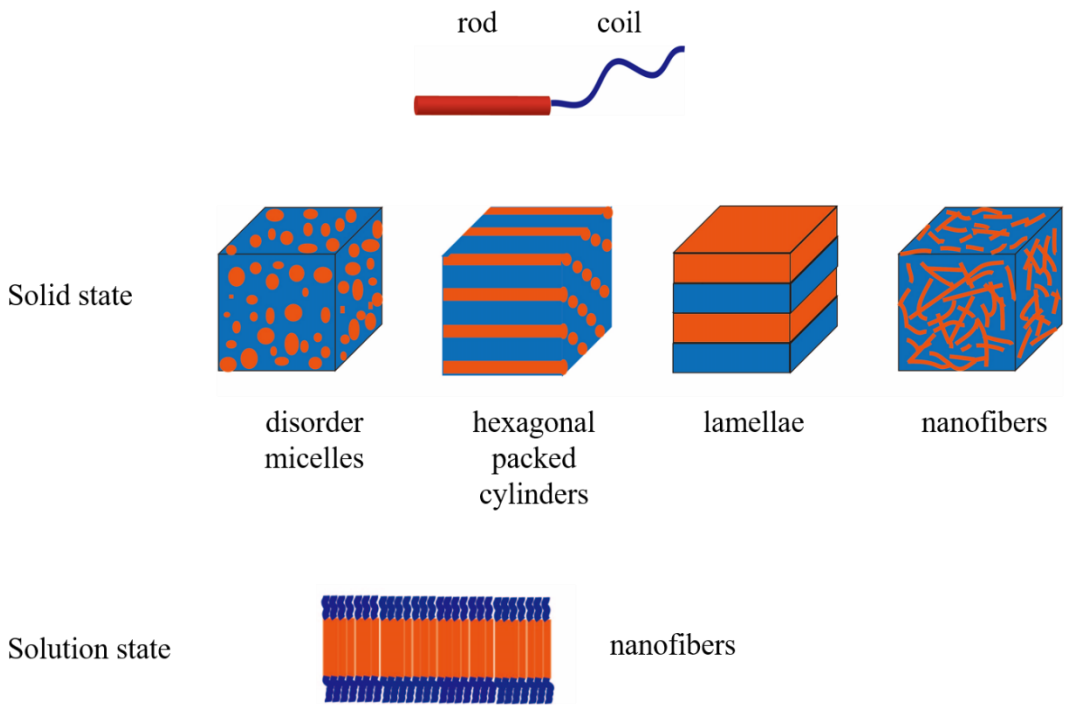

Figure 1.3: nanostructures formed from PT-coil copolymers

In addition, a competition between head-to-tail J-type aggregation and head-to-head H-type aggregation of conjugated polymers is an interesting aspect when considering physical performance of these materials[50,51] (Figure 1.4), especially in

photophysical spectra. For the P3HT linear chains, an HJ-aggregation was proposed[50]: inter- and intra- chain interactions are corresponding to H- and J- aggregation. For example, the spin-cast film by chloroform solution presents H-favor model when each polymer is regarded as chromophore in the π-stacking[51,52,53]; while the nanofibers from toluene shows J-favor model due to the strong intra-chain interactions[54]. Based on the above result, various methods are used to understand and control these two aggregation[51-56]. Specifically, a transition from J-favor to H-favor aggregation can be controlled by using linear P3HT block copolymers: the J-aggregates P3HT nanofibers encapsulated by P3HT-b-PEO[57]; or by crosslinking poly(3-hexylthiophene)-block-poly(3-methanolthiophene) (P3HT-b-P3MT)[58]; or by simply controlling volumetric ratio of different solvent mixtures[41,59].

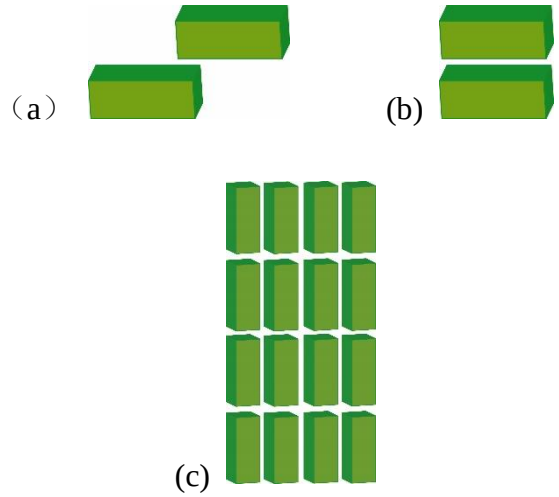

Figure 1.4: J-type aggregation (a), H-type aggregation (b) and HJ-aggregation model (c)

More morphologies are needed by synthesizing nonlinear P3HT copolymers, including graft (brush, comb), cyclic or star architecture. P3HT based amphiphilic

starlike copolymers[60] and P3HT-g-PEO[61] were synthesized and form micelle structures under controlled solutions. Besides, several groups started to focus on the brush polymer with P3HT as side chains. PNB graft copolymer with P3HT and fullerene side chains was first attempted by Fréchet[62]. In this copolymer, P3HT was synthesized with broader PDI by the nature of palladium catalyst[63,64], additionally, diblock copolymer showed multimodal SEC result[65]. S. Hilf later synthesized polynorbornene-poly(thiophene amides), which enabled limiting water soluble polythiophene derivatives as the side chain[66]; Z. Lin synthesized PS-g-P3HT via grafting P3HT to PS backbone via click reaction, resulting non-crystalline P3HT nanofibers[67]; S. Ahn and Dean van As synthesized polynorbornene-graft-poly(3-hexylthiophene), presenting an enhancing physical aggregation[68] and better electrical properties with long side chains[69], while the macromonomers were yet fully washed and the nanostructure was yet to obtained; T. Hayakawa and Y. Qiao observe honey cone structure and better mechanical properties[70,71] while only oligomeric P3HT with 3 repeating unit were studied.

Compared with linear copolymer, brush polymer containing P3HT as side chain can overcome aggregation, poor solubility and low mechanical properties from rigid backbone. Due to various interactions between block components, free energy balance can be better modulated while forming supramolecular structures. Additionally, due to the nature of the difference between rod and coil confirmation[25,72,73,74], different types of nanosturctures may be observed.

Based on previous work, our goal is to find out architectures obtained by dual

brush containing both P3HT (rods) and coils as side chain, and try to figure out possible unique structures. This goal includes two aspects: 1) design a synthetic routine to precisely control grafting density, molecular weight (Mw) and polydispersity index (PDI) of brush polymer; and 2) understand their architecture correlations and finding out whether unique structures can be obtained. From known synthetic methods, we can reach the first aim and by changing different conditions we may find out the answer for the second aim.

In this thesis, we report synthesis and characterize amphiphlic diblock graft copolymer [Polynorbornene-graft-Poly(3-hexylthiophene)]-block-[polynorbornene-graft-Poly(ethylene oxide)] [(PNB-g-P3HT)-b-(PNB-g-PEO)] (P3HT-PEO) and their architectures in solutions. In the second chapter, we describe the synthesis of that polymer via Grignard reaction, “click reaction” and ring opening metathesis polymerization (ROMP); in addition, melt study was performed. In the third chapter, we investigate properties of brush polymers and discuss the result.

Chapter Two

SYNTHESIS OF BRUSH POLYMER CONTAINING P3HT AS SIDE CHAINS

2.1. Introduction

Precise designing brush copolymers requires a well-controlled synthesis. It involves in definite molecular weight (MW), small PDI and grafting density. Three approaches are defined based on the mechanism: grafting from[75,76] , grafting to[77,78,79] and grafting through[80,81,82,83] (Figure 2.1). “Grafting from” involves in initiation sites on the polymer backbone (macrointiator) and monomers of side chains while “Grafting to” is approached by side-functioned backbone and polymers used as side chains. “Grafting through” is employed via polymerization of macromonomers. Compared with “grafting from” and “grafting to”, “grafting through” can better control grafting density, PDI of the side chains and the length of backbone. It’s also easier to wash off impurities in the synthesis, therefore, it’s commonly used in designing dual brush.

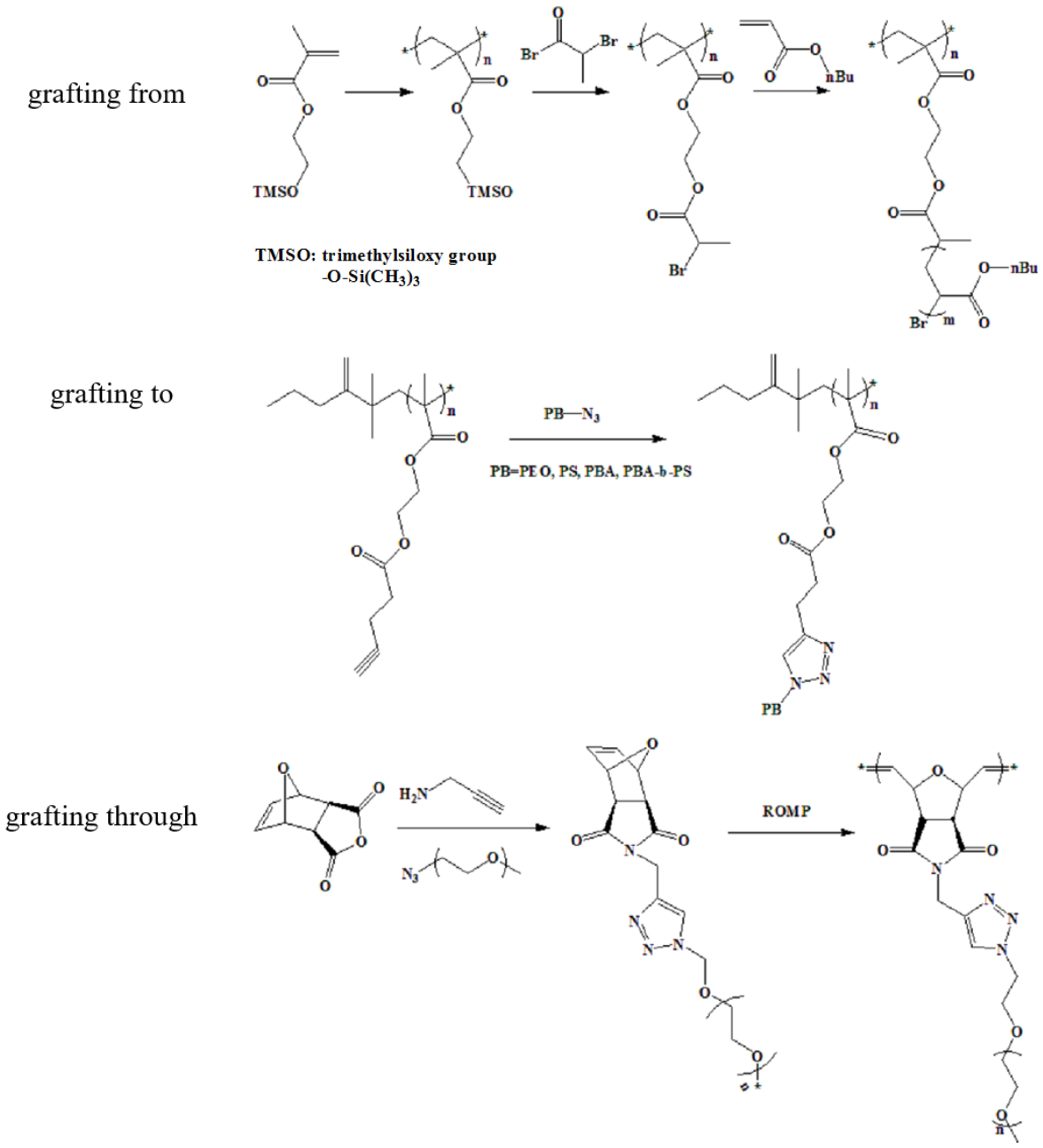

Figure 2.1: 3 ways to make brush copolymer[75, 77, 80]

Ever since the invention of Grubb's catalyst, ROMP provides effective way to obtain brush polymer via "grafting through" [80,81,82,83]. Atom transfer radical polymerization (ATRP)[84,85,86], nitroxide mediated radical polymerization (NMP)[76], anionic polymerization[87,88,89,90,] and Reversible Addition-Fragmentation chain Transfer (RAFT)[91,92] are widely explored to make macromonomers, but those reactions cannot

well-establish norbornene-P3HT macromonomers due to the hash synthesis requirement of P3HT.

Our goal is to synthesize brush via grafting “through method”. High efficient “click reaction” [80,93,94,95,96,97,98] is one of the solutions since end-functioned P3HT can be achieved by Grignard Reaction[99,100,101].

From ROMP, Grignard reaction and “click reaction”, we design synthesis procedure as shown by Figure 2.2. Grignard reaction was introduced to synthesize P3HT end functioned with alkyl with low PDI in step 1; and then norbornene was linked to P3HT via “click chemistry” with high efficiency in step 2 and step 3; and finally, brush was made via ROMP in step 4.

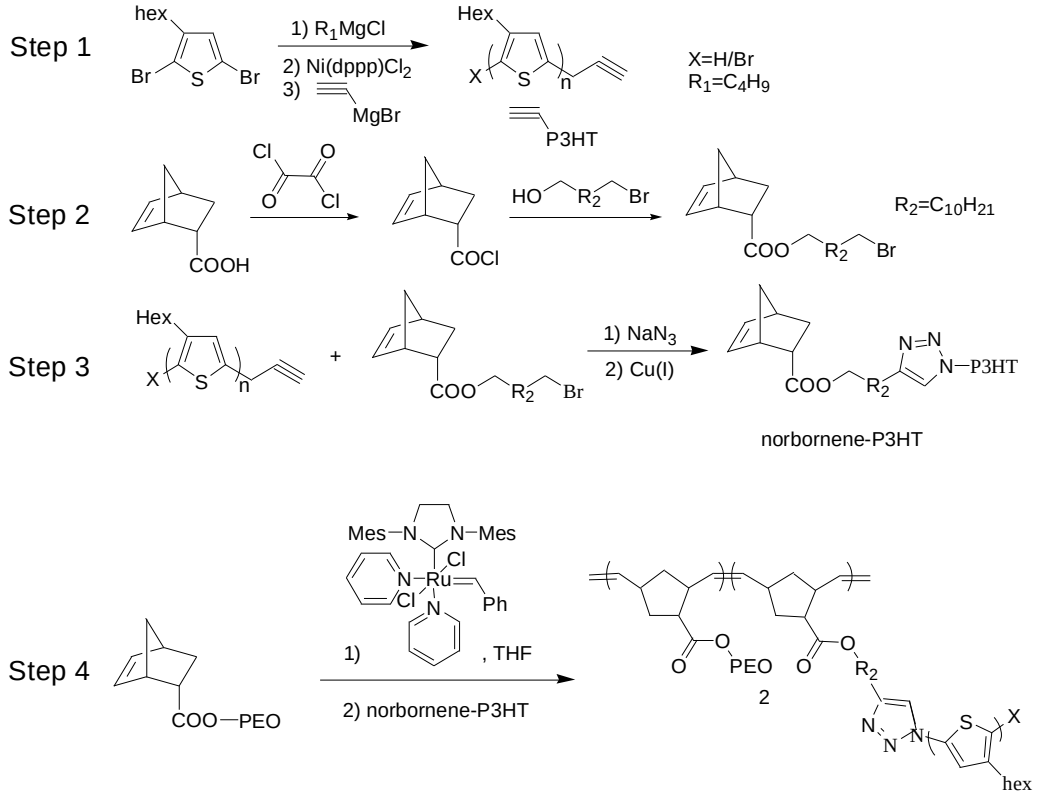

Figure 2.2: Synthesis of brush block copolymers

2.2. Materials

2,5-dibromo-3-hexylthiophene, [1,3-bis(diphenylphosphino)propane] nickel(II) [Ni(dppp)Cl_2], copper(I) bromide (95%), N,N,N',N'-pentamethyldiethylenentriamine (PMDETA), n-butylmagnesium chloride (2M, diethyl ether), 12-bromo-1-norbornenedodecane, ethynylmagnesium chloride (0.6M solution in THF/Toluene), poly(ethylene oxide) methyl ether (PEO, 2000mg/mol), oxalyl chloride, Grubb's catalyst second generation (1,3-Bis(2,4,6-trimethylphenyl)-2-imidazolidinylidene)dichloro(phenylmethylene)(tricyclohexylphosphine)ruthenium (G2) and 5-nornornene-2-carboxylic acid (NBCOOH) were purchased commercially from sigma-aldrich and Fisher. Anhydrous tetrahydrofuran (THF, 99%, Acros) was purged with nitrogen for 30min before use. Modified Grubbs' second catalyst and norbornene poly(ethylene oxide) (NBPEO) (Figure 2.3) is prepared by literature[81]. All other reagents were purchased from commercial sources and used without further purification.

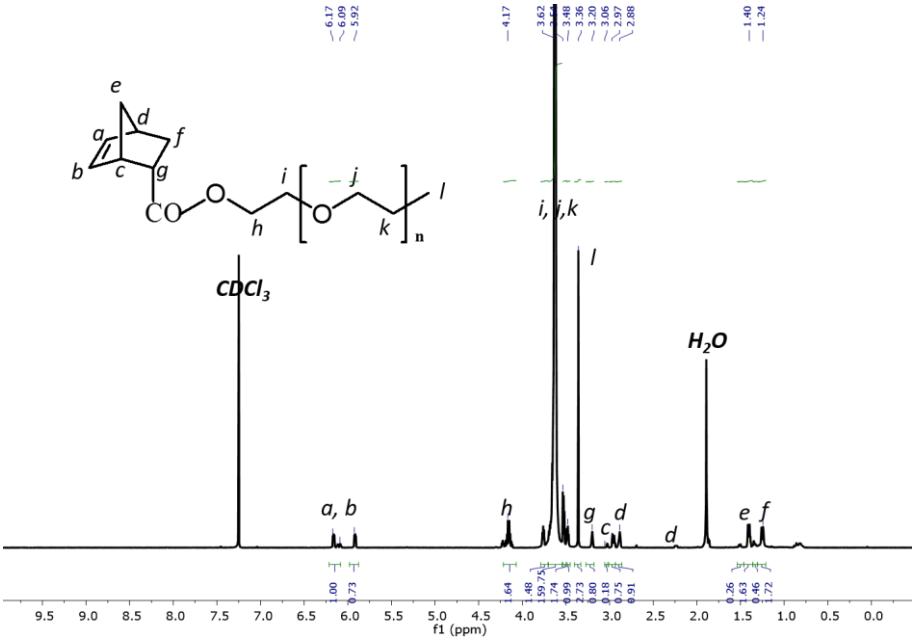

Figure 2.3: H[1]NMR of NBPEO

2.3. Macromolecular characterization of NBCOCl, NBP3HT, NBPEO, PNB-g-P3HT and (PNB-g-P3HT)-b-(PNB-g-PEO)

[1]HNMR and [13]CNMR spectra were obtained by Bruker DMX 400MHz NMR spectrometer under room temperature with $CDCl_3$ as solvent. 7.24 ppm is the peak of $CDCl_3$ is the internal standard. Molecular weight and polydispersity indices (PDI) were determined by gel permeation chromatography (GPC) equipped with Jordi Gel fluorinated DVB columns (1-100K, 2-10K & 1-500Å) PL-ELS1000 evaporative light scattering (ELS) and a Waters 2487 dual wavelength absorbance detector UV-Vis detector with THF as eluent and polystyrene as standard at room temperature. Mass spectra of NBCOCl methanol solution was confirmed by AccuTOF-DART(JEOL).

2.4. Synthesis of alkynyl-functionalized poly(3-hexylthiophene) (P3HT)

In an oven-dried 250ml flask, 4.9g of 2, 5-dibromo-3-hexylthiophene was dissolved in 150ml of anhydrous THF and 7.5ml of butyl magnesium chloride was subsequently added for 12h. Then, (1) 0.75g of Ni(dppp)Cl_2 was added and stirred for 15min and (2) 30ml of 0.5M ethynylmagnesium chloride was then added and the solution was stirred for 15min to terminate the reaction. alkynyl-functionalized poly(3-hexylthiophene) was obtained by precipitation from methanol. The polymer was purified by Soxhlet extraction with methanol. Dark red powder. Yield: 73%. Mn(GPC) is 4227g/mol with PDI as 1.14. ^{1}HNMR (400MHz, $CDCl_3$), δ): 6.96(s, 1H, cyclic, -CH=C-), 3.48(s, 1H, -C≡CH), 2.78(t, 2H, -CH_2-C=CH), 1.68 (m, 2H, -CH_2-CH_2-CH=C-), 1.31 (m, 6H, -CH_2-), 0.88 (m, 3H, -CH_3); (Figure 2.4)

2.5. Synthesis of 12-bromo-1-norbornenedodecane (NBBr)

NBCOOH was treated with excess oxalyl chloride to get norbornene carbonyl chloride (NBCOCl). 0.5M of 12-bromo-1-dodecanol THF was added to dry NBCOCl at 1:5 molar ratio. After stirring for 12h, the product was precipitated from diethyl ether. Pure solid product (NBBr) was obtained after freeze drying. Transparent liquid. Yield: 85%. ^{1}HNMR (400MHz, $CDCl_3$), δ): 5.9-6.2(m, 2H, cyclic, -CH=CH-, endo/exo), 3.99 (m, 2H, linear, -COO-CH_2-), 3.38(t, 2H, -CH_2Br), 2.18-3.20(m, 3H, cyclic, -CH-, endo/exo), 1.25-1.83(m, 8H, -CH_2-), 1.25 (m,12H,cyclic, -CH_2-, endo/exo); AccuTOF-MS (m/z) calcd 385.3848 found [MH^+]=387.1724; (Figure 2.5, Figure 2.6 and Table 2.1)

2.6. Synthesis of norbornenyl P3HT (NBP3HT)

NBP3HT was synthesized via click reaction[102]. 135mg of sodium azide was treated with 40ml 0.025M 12-bromo-1-norbornenedodecane in THF at 35◦C for 3h to produce norbrornene azide. In the next step, 200mg of P3HT, 6mg of Cu(I)Br, 34mg of N,N,N′,N′,N″-pentamethylethylenetriamine(PMDETA) THF solution was added into nitrogen purged reaction flask and stirred for 5h under 40◦C. Polymer is obtained by precipitation with methanol and purified by Soxhlet extraction. Dark black powder. Yield 70%. Mn(GPC) is 1849g/mol with PDI as1.22. ^{1}HNMR (400MHz, $CDCl_3$), δ): 7.67(s, 1H, triazole), 6.93(s, 1H, cyclic, -CH=C-), 5.94-6.22(m, 2H, cyclic, -CH=CH-, endo/exo), 4.06(d, 2H, -CH_2-triazole), 3.97(m, 2H, linear, -COO-CH2-), 2.75(t, 2H, -CH_2-C=CH), 2.15-3.20(m, 3H, cyclic, -CH-, endo/exo), 1.20-1.97 (m, 22H, -CH_2-,), 0.840(m, 3H,-CH3); (Figure 2.7)

2.7. General procedure for synthesis of PNB-g-P3HT and (PNB-g-P3HT)-b-(PNB-g-PEO) (P3HT-PEO)

A representative synthetic procedure for the preparation of (PNB-g-P3HT)-b-(PNB-g-PEO) is described here. A dried reaction vessel was charged with 250mg of NBPEO (2000g/mol) THF solution. 7mg of modified Grubbs 2nd generation catalyst was then added and stir for 30min. Then, 30mg of NBP3HT was mixed for 8h under 35◦C. An excess of 1ml of ethyl vinyl ether (EVE) was used to terminate the reaction. The final product is purified under the silica gel column and dried under evaporation. The actual ratio between P3HT side chain and PEO was calculated by integration ratio of peak at 6.94ppm (P3HT) and peak between 3.70-3.20 ppm (PEO). Dark red powder.

Yield: 60%. Mn(GPC) is 19222g/mol with PDI as 1.26. ^{1}HNMR (400MHz, $CDCl_3$), δ): 6.94 (s, 1H, cyclic, -CH=C-), 5.50-5.00(m, 2H, -CH=CH-, endo/exo), 3.70-3.20(m, 30H, $-CH_2CH_2O-$), 2.75(t, 2H, -CH2-C=CH), 1.20-1.80 (m, 22H, $-CH_2-$,), 0.85(m, 3H,-CH3); (Figure 2.8-Figure 2.10)

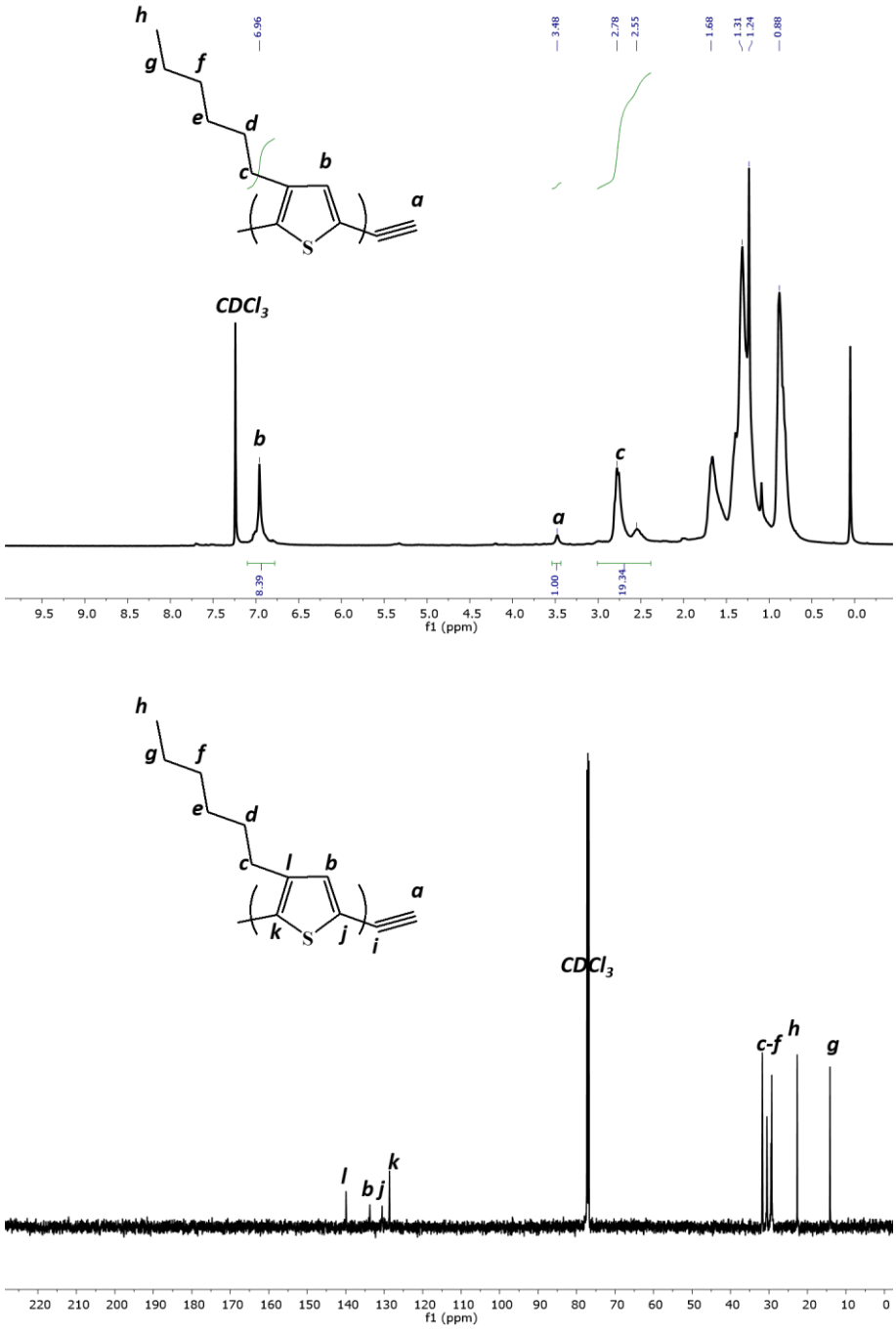

Figure 2.4: H1NMR and C13NMR of P3HT

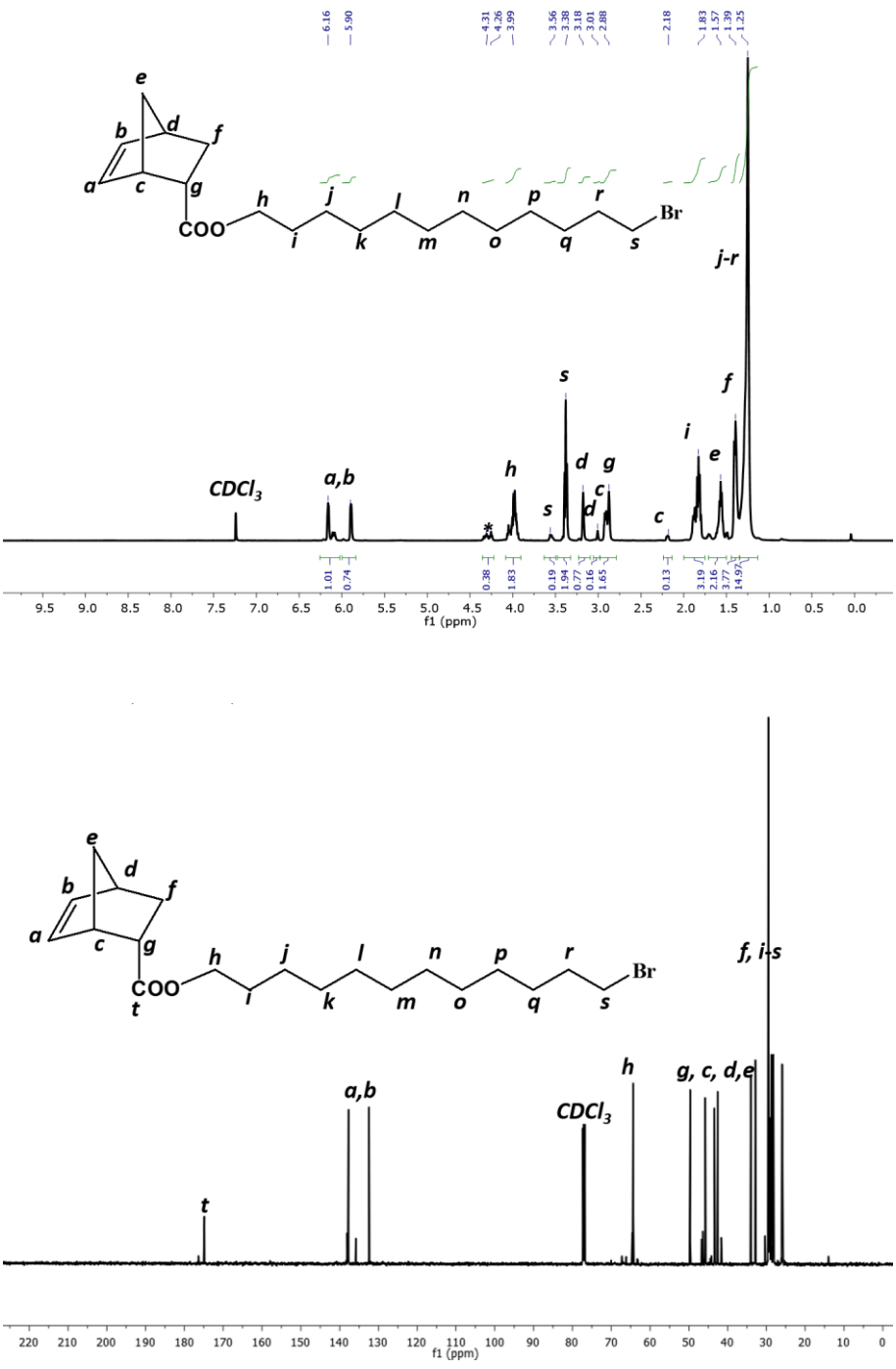

Figure 2.5: H^{1}NMR and C^{13}NMR of NBBr

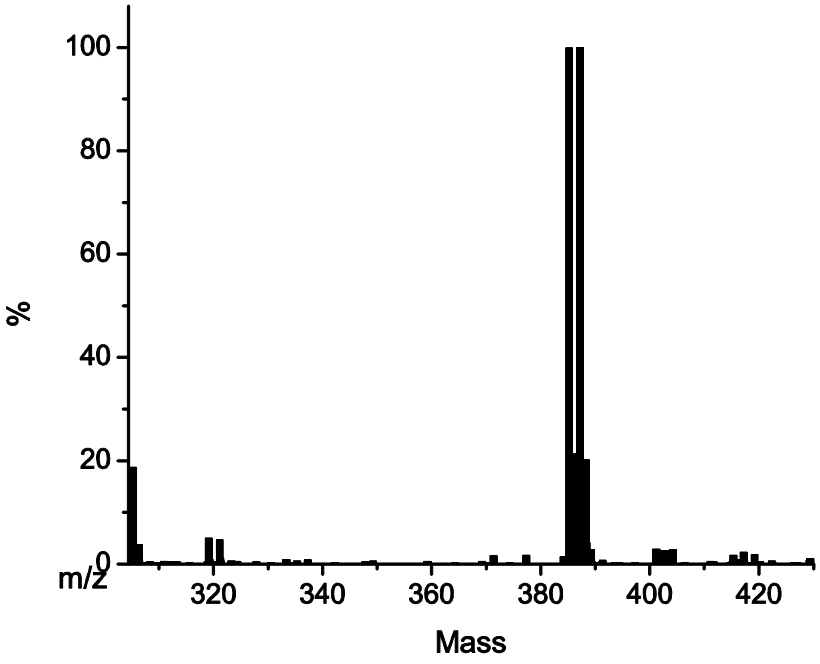

Figure 2.6: MS of NBBr

Mass	Fragmentation
282.2832	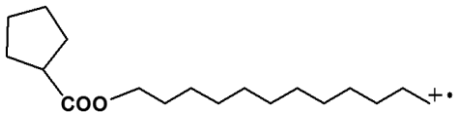
305.2510	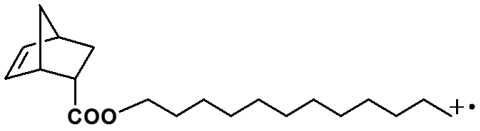
319.1245	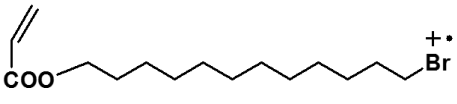

321.1259	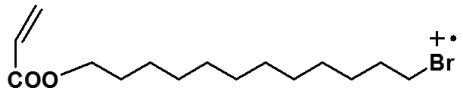
385.1727	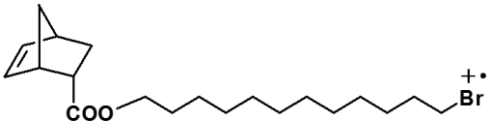
387.1720	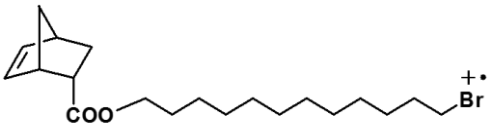

Table 2.1: Major fragmentations of NBBr in MS

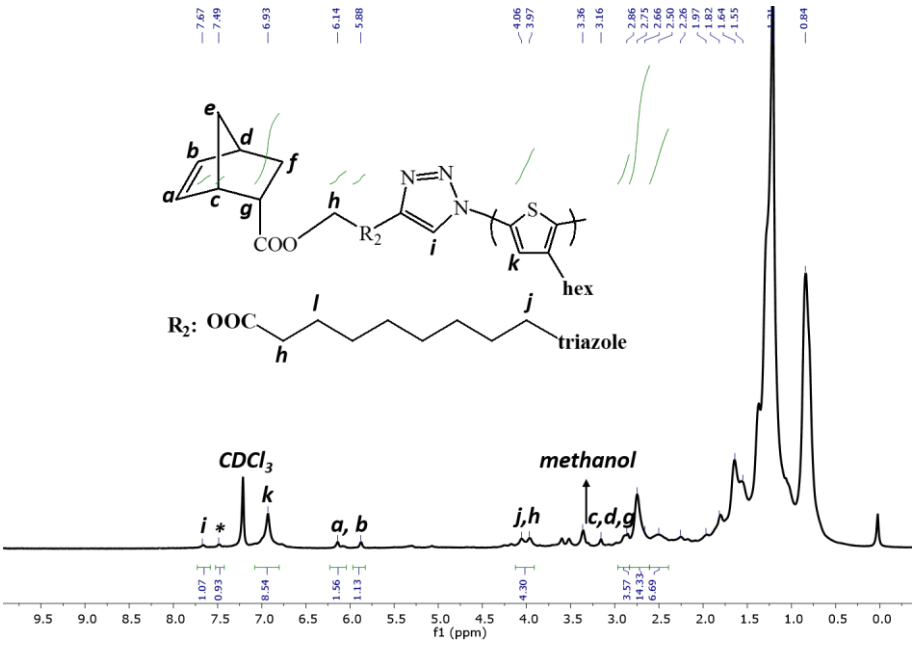

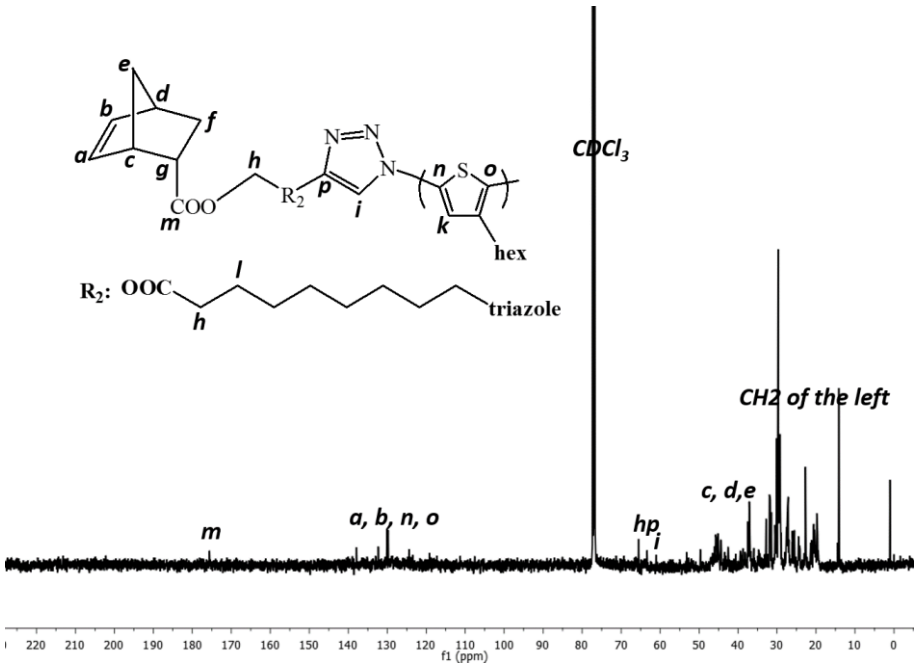

Figure 2.7: H^{1}NMR and C^{13}NMR of NBP3HT

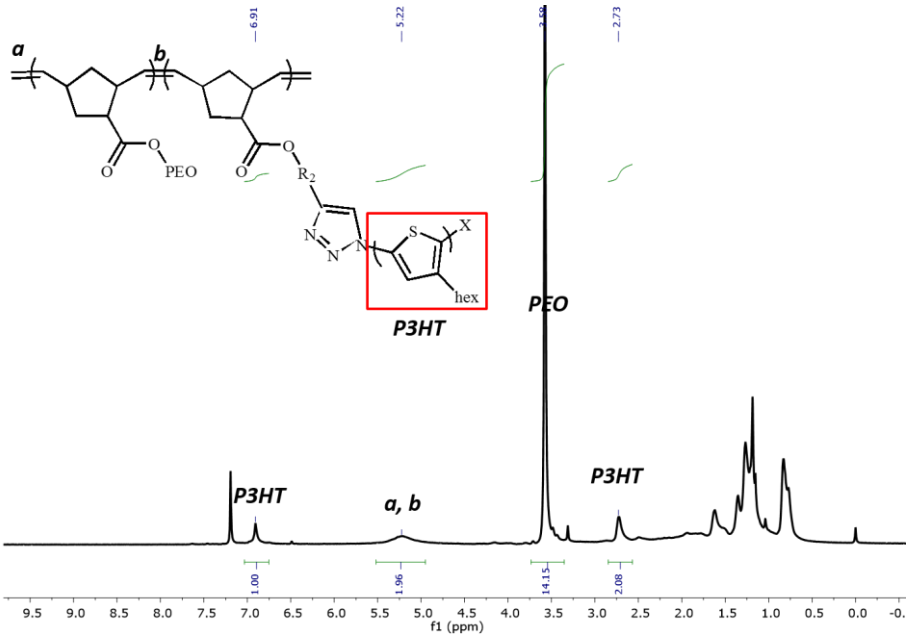

Figure 2.8: H^{1}NMR P3HT-PEO

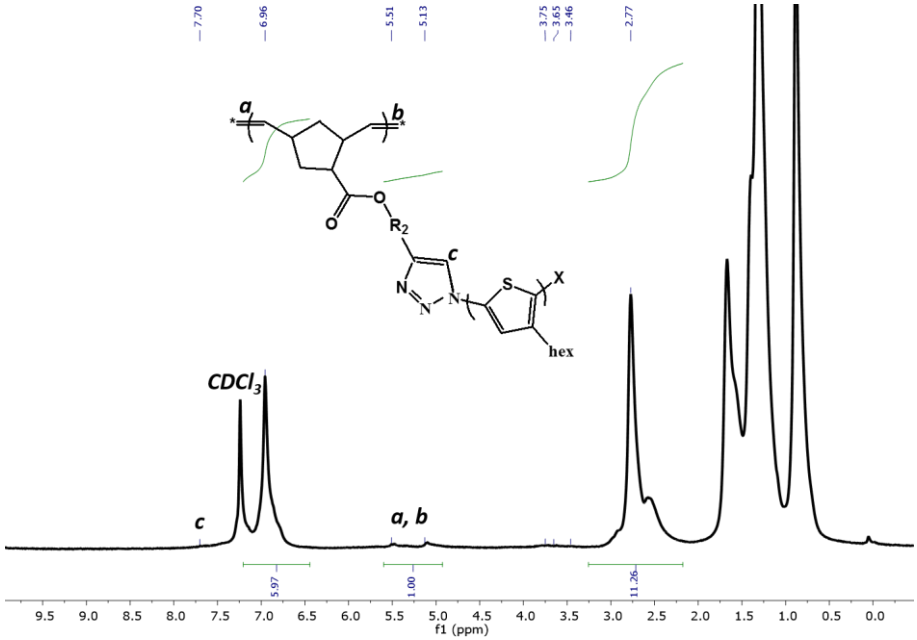

Figure 2.9: H^1NMR of PN-g-P3HT$_5$ (ROMP5)

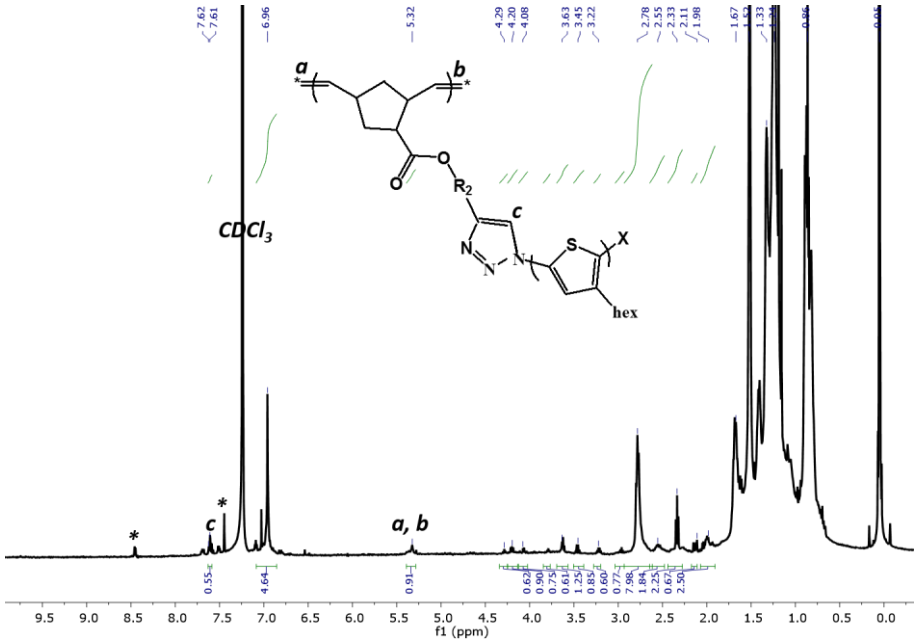

Figure 2.10: H^1NMR of PN-g-P3HT$_{10}$ (ROMP10)

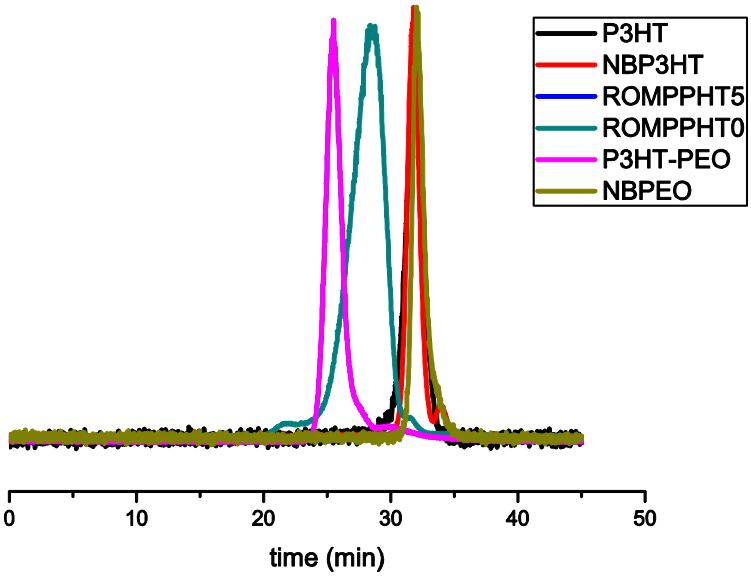

Figure 2.11: GPC traces of all the polymers

	Mn(g/mol)[a]	Mn(g/mol)[b]	PDI
NBPEO	3285	2000	1.1
P3HT	4227	1450	1.14
NBP3HT	1849	1773	1.22
ROMPP3HT5	10487	8866	1.03

ROMPP3HT10	19222	17732	1.26
P3HT-PEO[c]	49616	37732	1.29

Table 2.2: MW and PDI of polymers: [a]MW is obtained via GPC; [b] MW was obtained via the calculation of NMR; [c] [P3HT]:[PEO]=1:1 in the synthesis

2.8. Thermal properties

2.8.1 X-ray scattering

P3HT and PEO are both semicrystalline polymers. Therefore, crystalline peaks can be observed by X-ray scattering (Figure 2.12).

To obtain WAXS profile, powder X-ray diffraction instrument Scintag 2000 powder XDS with CuKα X-ray source（λ=1.542 Å）was used, a beam of 45 kV voltage and 40 mA current were set. Powdery sample (20 mg) was loaded on a designed glass holder and data was collected with 2θ range 2-35° with a step scanning rate of 0.02°/min.

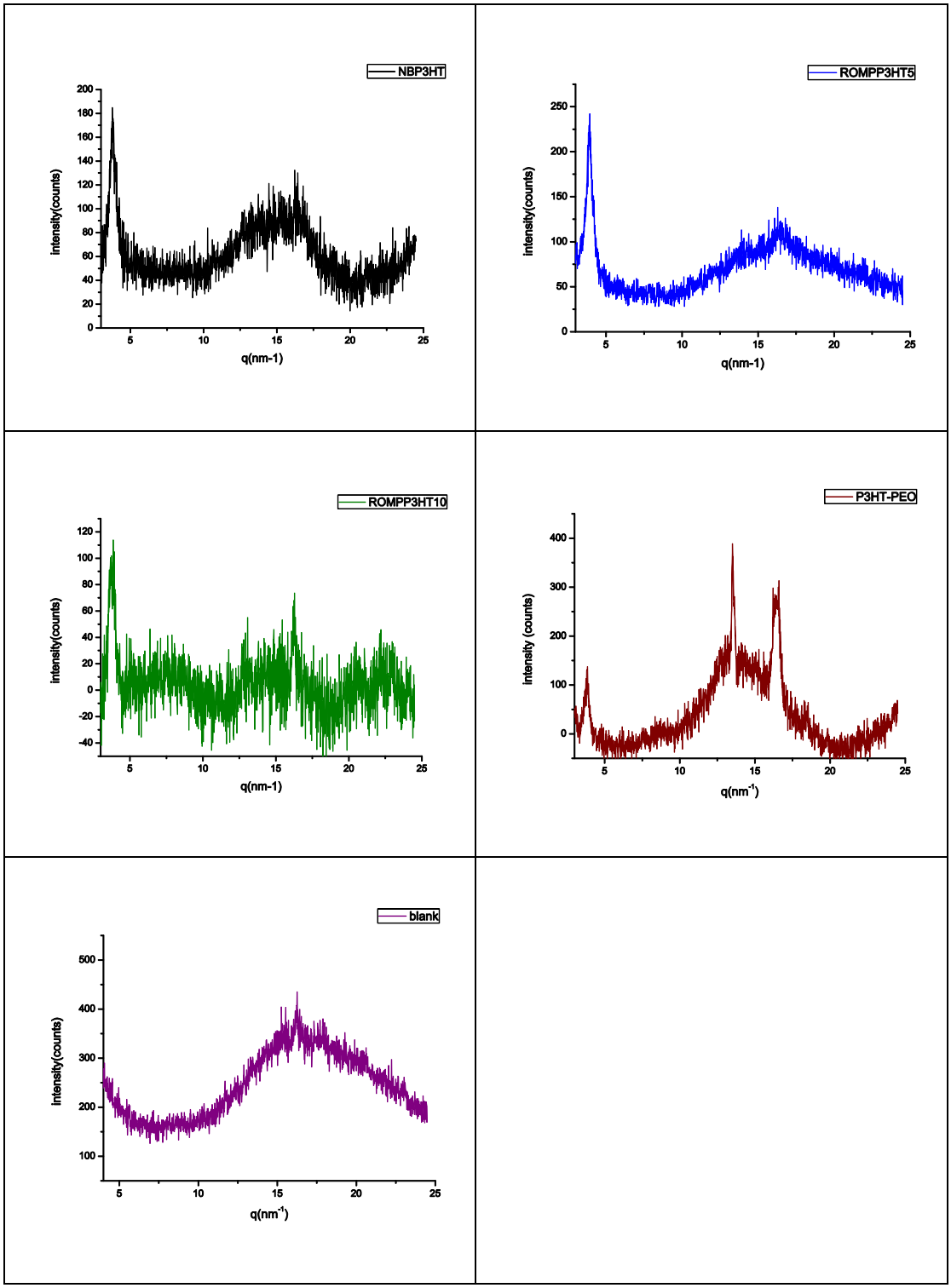

Figure 2.12: WAXS patterns of NBP3HT (black line), ROMPP3HT5 (blue line), ROMPP3HT10 (green line), P3HT-PEO (brown line) and blank (purple line) under room temperature

For linear P3HT packing as crystals, it is reported to show parallel stacks of

polymer main chains while hexyl side chain forms the space between main chains[103]. P3HT peak was observed at q~4.0nm^{-1} and broad peak between 10-20 nm^{-1} was attribute to disorder of side chain and hexyl spacer[103]. In P3HT-PEO, sharp peaks range from 13-17nm^{-1} indicates PEO crystals.

2.8.2. Thermal Analysis

TGA results were obtained by using TA Instruments TGA Q-500. Around 40-50mg of solid sample was placed in a platinum plate with heating rate of 10◦C/min. Results were analyzed by TA Universal Analysis software.

TA-2920 DSC (Q-200 series) was used to test thermal properties of polymers. Indium standard was used for calibration by TA Universal Analysis software. Solid sample was 5-10mg with scanning rate with 20◦C/min. Phase transition temperatures were determined in the first or second cooling cycle scan.

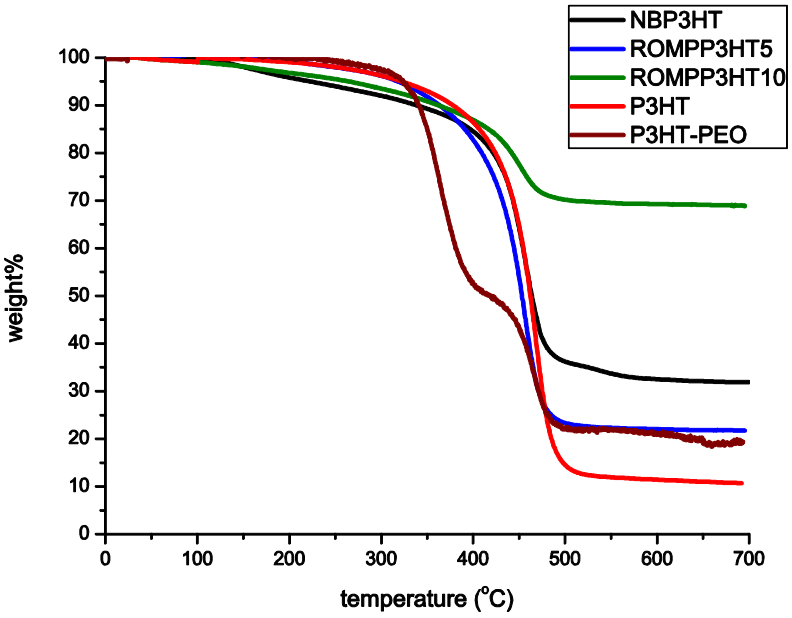

Figure 2.13: TGA of polymers

An obvious less weight loss of ROMPP3HT10 was observed which may come from crosslink of polymer. When EVE terminated ROMP, vinyl-end was formed in one-end. Relative low molecular weight of brush lead these vinyl-end may fast thermally crosslink when temperature arise[104] while P3HT aggregates via intramolecular interactions. However, in ROMPP3HT5 brush, due to the small DP of backbone, alkyl spacer can be regard as side chain in brush, resulting to core-shell or double cylinder block brush copolymer[105,106,107]. Entangled coil alkyl spacer hindered vinyl group exposed with each other, forming intermolecular π-π aggregation. This vinyl hindrance in dual brush can also be explained by the entanglement of PEO, resulting only crosslinking of ROMPP3HT10.

P3HT started to decompose at temperature around 350℃. We expected to observe

similar trend at similar temperature. However, NBP3HT and brushes started to have weight loss at around 150℃, indicating decomposition of polymer chains. This phenomenon was further proved by DSC: P3HT melting peak at 215℃ was only observed in P3HT DSC curve, flat lines showed up in NBP3HT, ROMP5 and ROMP10 and only PEO crystalline peak was observed in P3HT-PEO. We believe the abnormal disappearance of P3HT melting peak may come from decomposition of NBP3HT before melting, yet the reason of it remains unknown. In addition, this unknown reason may also impact fast degradation of those polymers (Figure 19) even though they are stored in fridge.

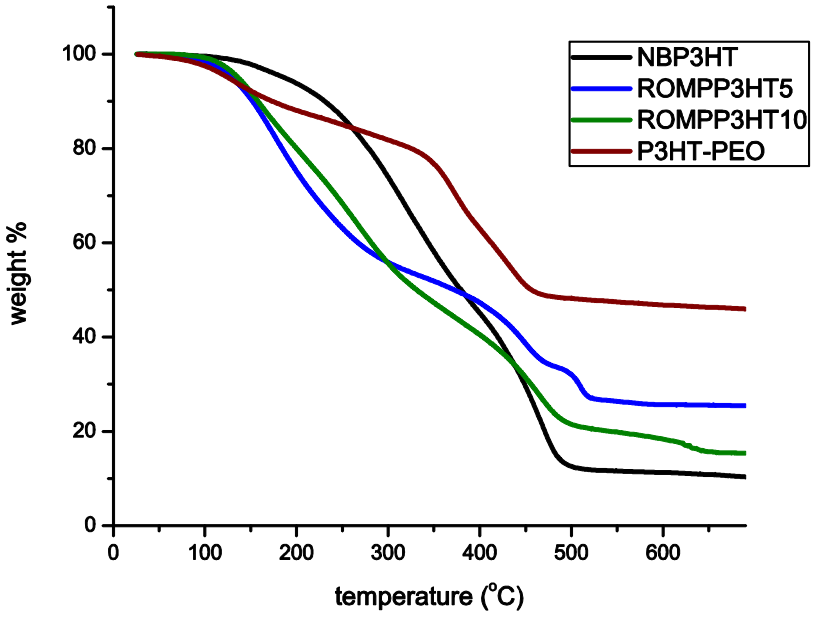

Figure 2.14: TGA of polymers after 3 months of storage

In conclusion, we successfully synthesized well-controlled brush polymer with designed grafting density, Mw and low PDI. However, unknown degradation was found

before expected degradation temperature and therefore no nanoscale architectures in solid can be obtained because it will decompose before reaching melting temperature. We can only observe structures in solutions.

Chapter Three

SOLUTION PROPERTIES

3.1. Introduction

Ever since dual brush polymers are synthesized and characterized[108,109,110,111,5,112,113,114] , dual brush polymers share similar properties with simple brush polymers: 1) the repulsive force of side chain strengthen the main chain, causing semirigid backbone and resulting in wormlike confirmation; 2) side chain confirmation is irrelative with chain length and contour length; 3) crystalline behavior is dominated by side chains[5,115,]; 4) lamella structures were mainly observed [98,5,116,117] while sphere and cylinders were also found[6,7] in melts; and 5) micelle[110,118,8,119,120,121] and tadpole[122] structures were observed in solution. However, most of dual brush block copolymers indicate the unique properties: 1) symmetry of the polymer including the length of side chain and backbone impact the forming of architectures[98,5,9,10,123,124]; 2) domain size are impacted by cross-sectional area between the two side chains[5,] 3) flower-like, dumbbell-like and Y-junction structures can be formed[122,9, 10, 125].

Even though, the less entangled side chain in those above brush polymers may result in semi-rigid polymers, the rigid nature and self-packing of rod side chain may lead to the difference between coil side chains. For example, solvent effect can be eliminated, speeding up the organization of microstructure[126,127]; confinement effect showed essential impact of confirmation[128] and ladder structures were observed[129].

Our goal of this chapter to find out structures in solutions. It may form different structure in solution than simple nanofibers even though strong aggregation occurs. We make this prediction because a new repulsion force may occur from close hexyl chain packing on thiophene ring, adding complexity of the structure.

In our polymer system, symmetric polymers are synthesized. Based on previous study, while explaining the phenomenon, alkyl spacer will also be considered which indicates more free rotation between main chains and side chains[130]. Due to the abnormal phenomenon of melt study, we use fresh made polymers for solution studies.

3.2. Photophysical properties

The photophysical properties of conjugated polymers can be understood by similar absorbance and fluorescence idea of chromophore aggregations from Kasha[131]. Neighboring coupling of chromophores is related to through-space Coulombic coupling, leading to negative coupling in J-aggregation and positive coupling in H-aggregation (in Figure 20, showing green exciton at the bottom of curvature in J aggregation and at the top of curvature in H-aggregation). Emission of Einstein phonons are strongly tendentious to the ground state (bottom black line in Figure 3.1) in J-aggregation while in H-aggregation, fast relaxation to lowest energy level lead to the change of phonon wave vector, resulting in a restriction of 0-0 coupling. The absorbance peak of J-aggregate will have red shift and peak of H-aggregates will have blue shift.

Even though energy gap between neighboring excited state tend to be zero as

conjugated polymer length increases, the presence of π-stacking delocalize electrons not only along a single chain but also between chains. This complex inter and intra-chain interactions cannot simply use red or blue shifting in optical spectrum to identify J- or H- aggregation, the ratio of I^{0-0}/I^{0-1} is a useful parameter, specifically in highly sensitive fluorescence spectrum, this number will decrease (increase) in J-aggregates (H-aggregates)[132, 50].

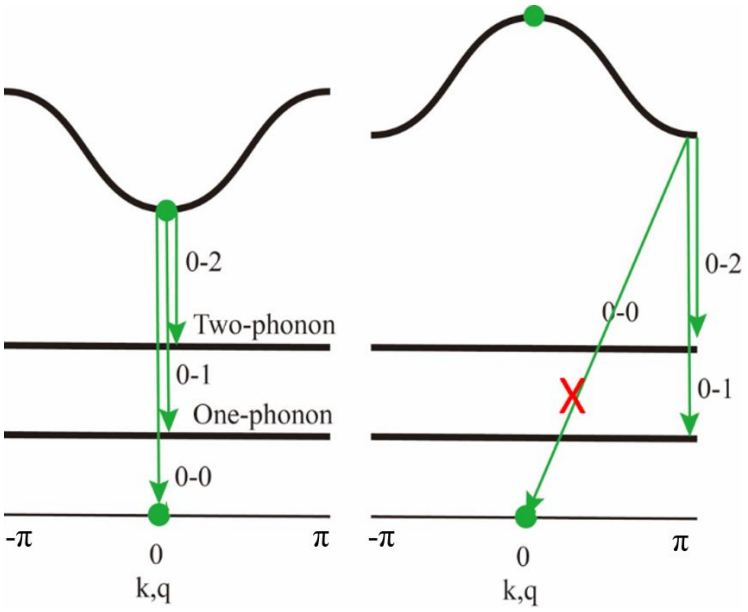

Figure 3.1: J-aggregation and H-aggregation emission

As it is discussed before, while in solution, the brush polymer itself contains both inter- and intra-chain interaction, in addition, due to aggregation of P3HT between side chains, it may not present coil conformation at the beginning. An interesting question then arises, when brush polymer dissolves in solutions, which interaction will take the leading role. And also, whether brush polymers share similar architectures as linear copolymers under the same solvent condition?

We select NBP3HT, ROMPP3HT10 and P3HT-PEO to find out the answer. To prevent precipitation, 0.3mg/ml of samples were prepared and was placed in a sealed cubic. Sensitive fluorescence spectrum Horiba Fluorolog III (PL) was set 25℃ in order to avoid temperature effect. Under excitation wavelength at 375nm, emission peak in spectrum comes from conjugated P3HT polymers. We pick up wavelength by choosing the highest intensity in the signal.

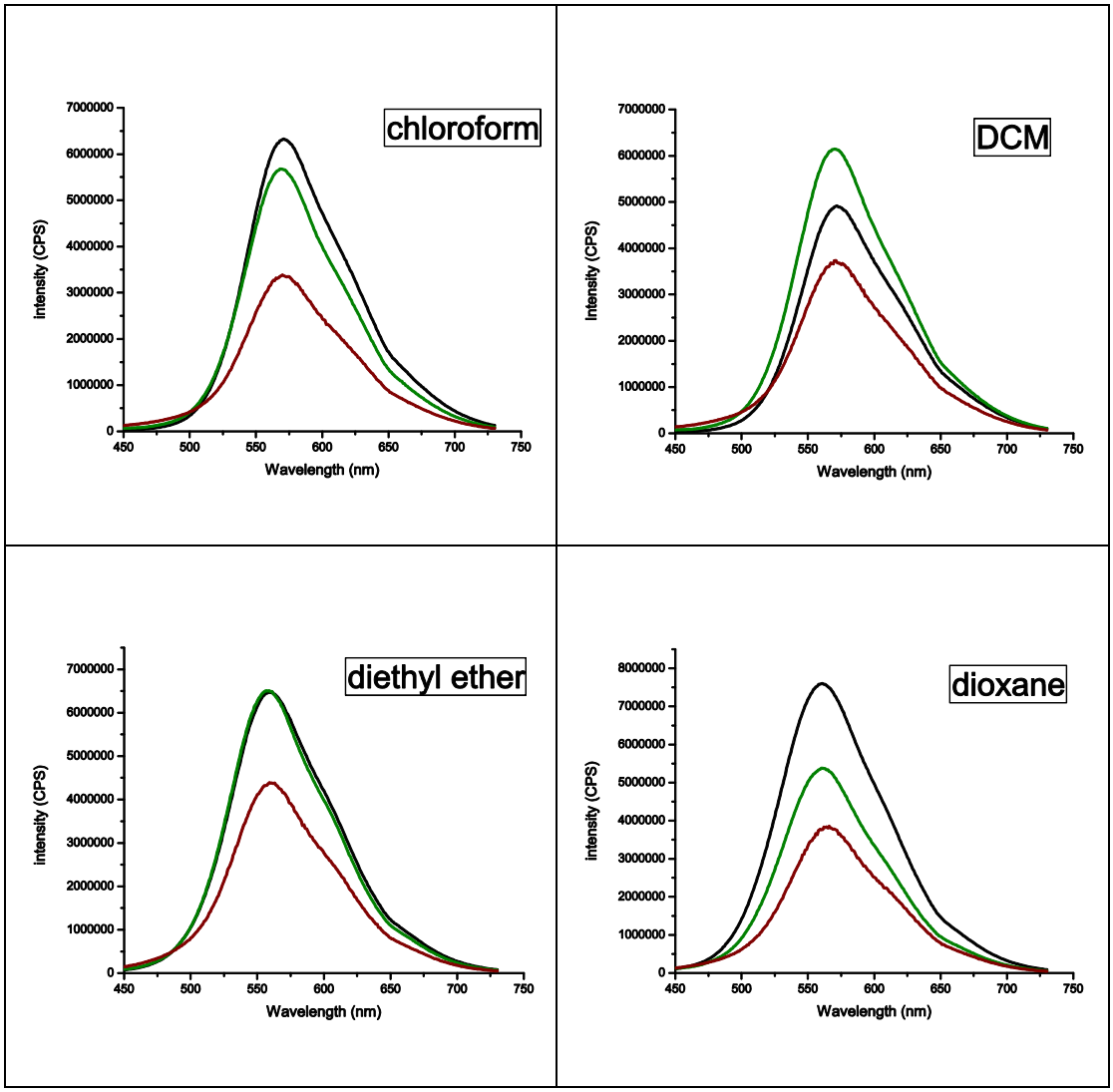

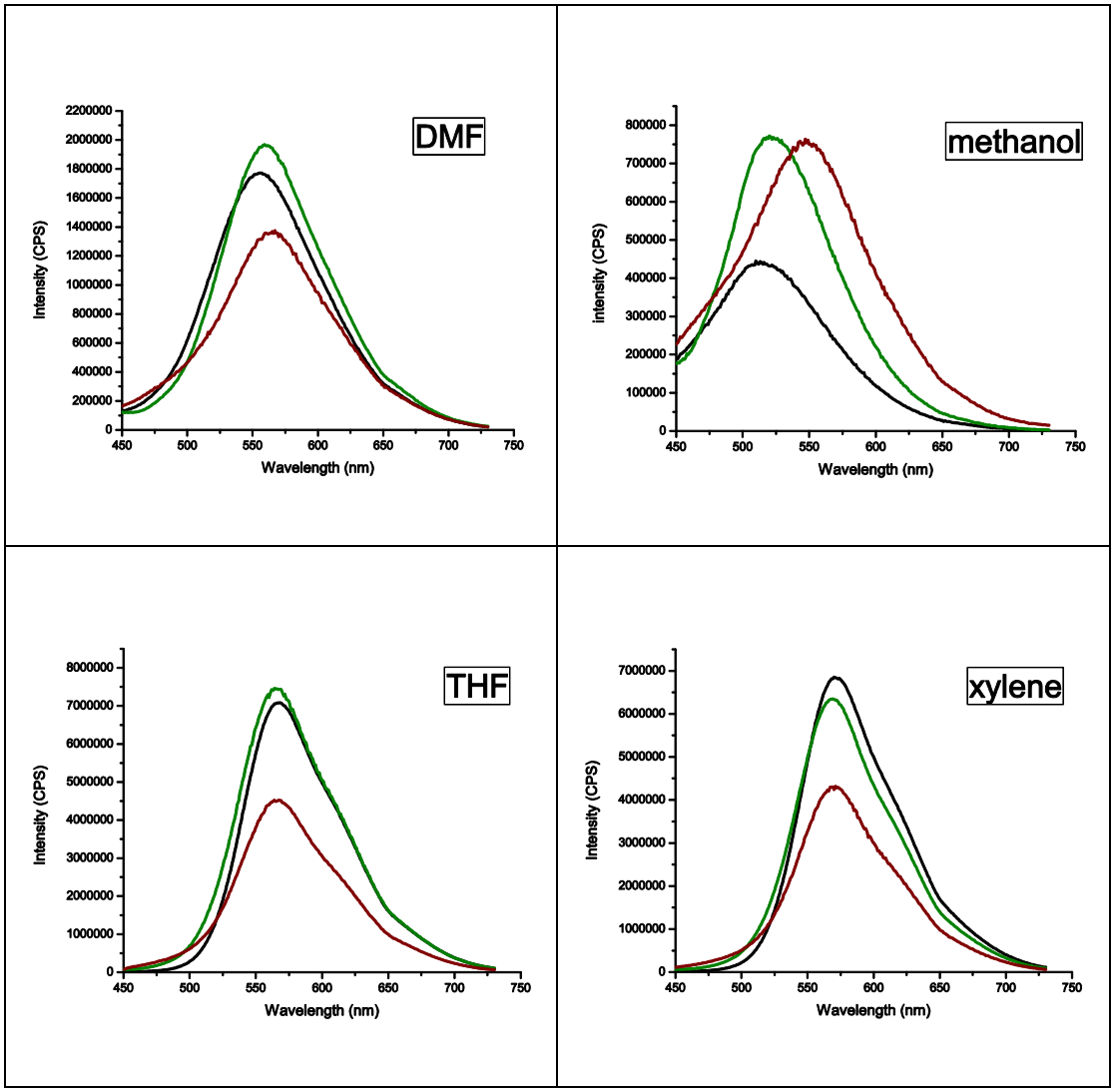

Figure 3.2: PL spectra of NBP3HT (black line), ROMPP3HT10 (green line), P3HT-PEO (brown line) under different solution

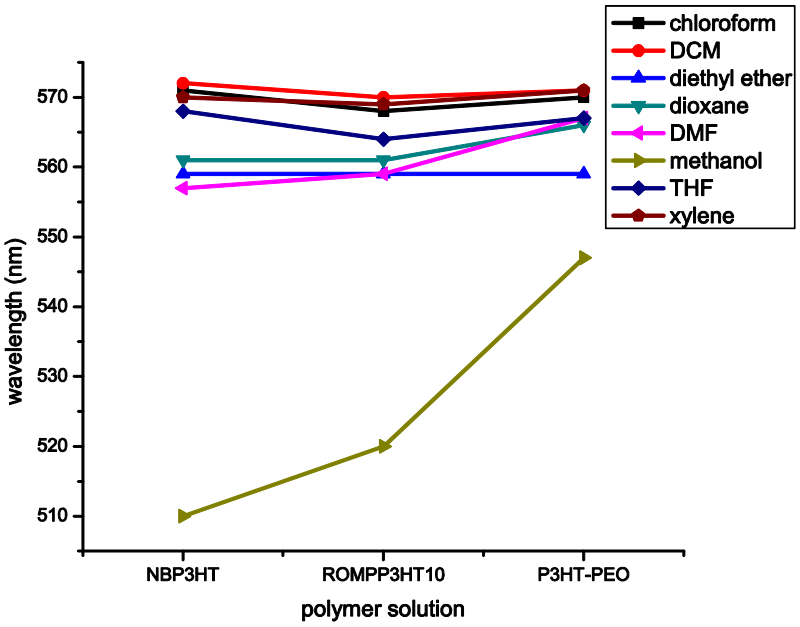

Figure 3.3: emission wavelength of NBP3HT, ROMPP3HT10 and P3HT-PEO in different solutions

Our first experiment is try to determine the types of solvent used in the later study (Figure 3.2, Figure 3.3). All those solvents can dissolve PEO; however, dioxane, dimethylformamide (DMF), diethyl ether and methanol are unfriendly solvents for P3HT while chloroform, dichloromethane (DCM), tetrahydrofuran (THF) and xylene are friendly solvents for P3HT. From Figure 22, we did not observe any more emission peaks in a single spectrum, indicating intrachain π-πtransition and also disordered aggregates of J-type polymers under room temperature[50, 133]. For most of solvents, there is little impact on emission wavelength among three polymer samples regardless of P3HT solubility, however, methanol makes the sharpest change in PL that may come from a coeffect of π-aggregation and supramolecular structure.

To begin with, time dependent PL under DCM was observed (Figure 3.4).

Emission wavelength of polymers have slightly changes, providing a small aggregation driven by crystallization of P3HT[45,41]. Among these three samples, ROMP10 shows most stable trend compared with NBP3HT and P3HT-PEO.

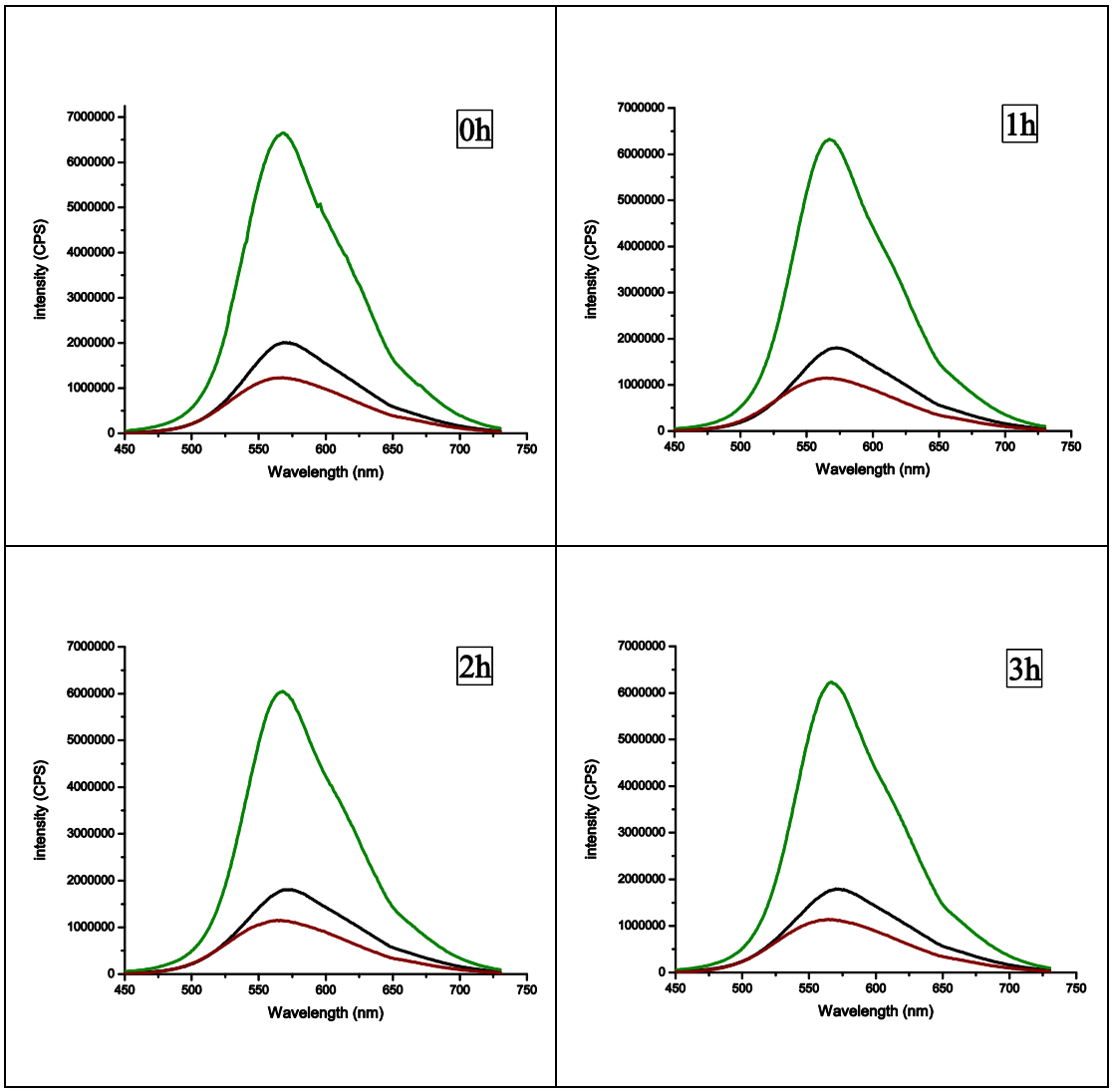

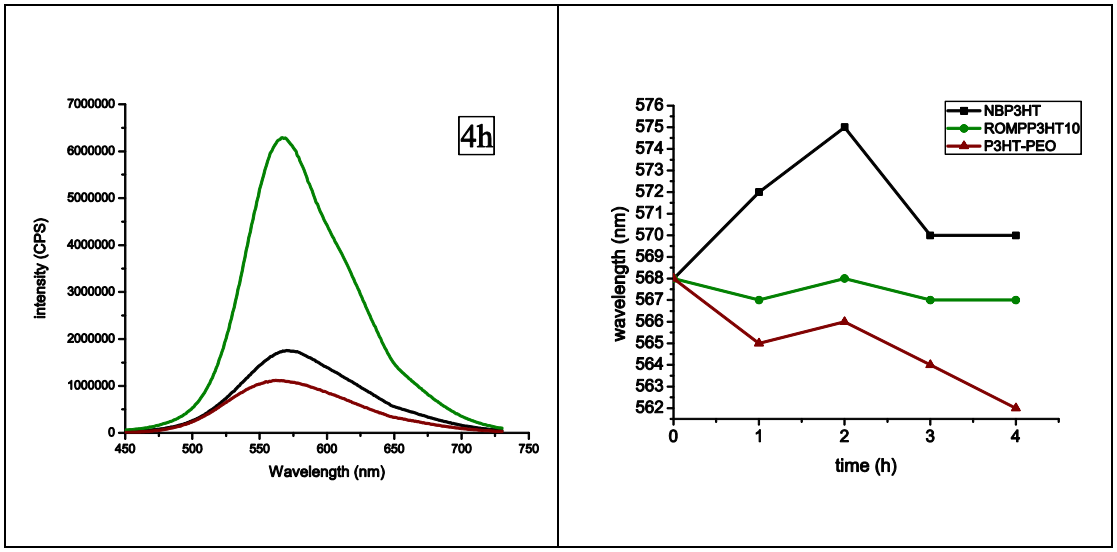

Figure 3.4: PL spectra of NBP3HT (black line), ROMPP3HT10 (green line), P3HT-PEO (brown line) in DCM solution by time

The change of wavelength is more obvious by adding more methanol in solution (Figure 3.5, Figure 3.6, Figure 3.7): 1) the initial wavelength of each types of polymers becomes different with each other and 2) when %DCM reaches 90%, precipitation will show up in NBP3HT and ROMP10 while P3HT-PEO solution remains homogeneous.

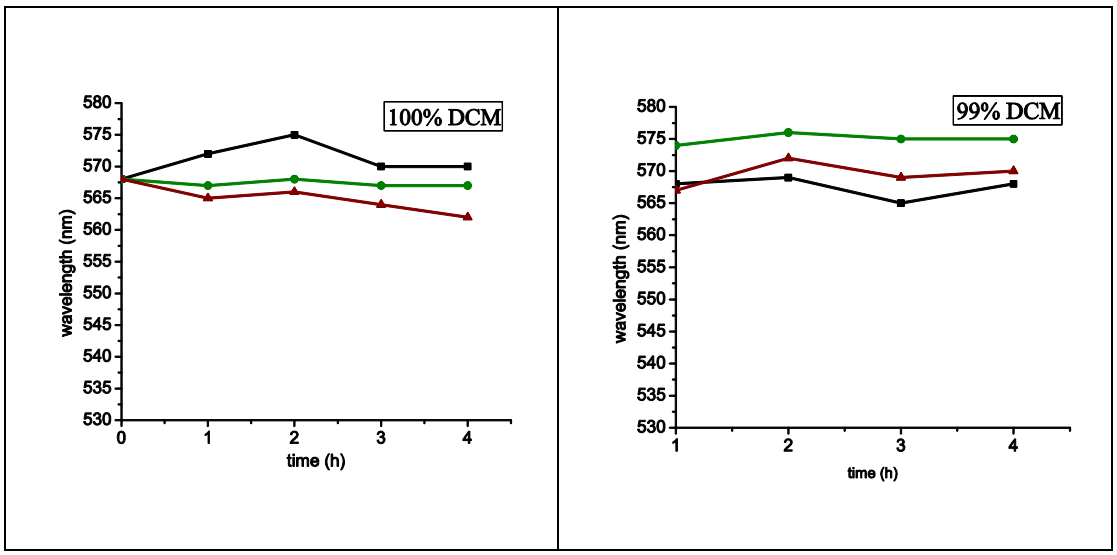

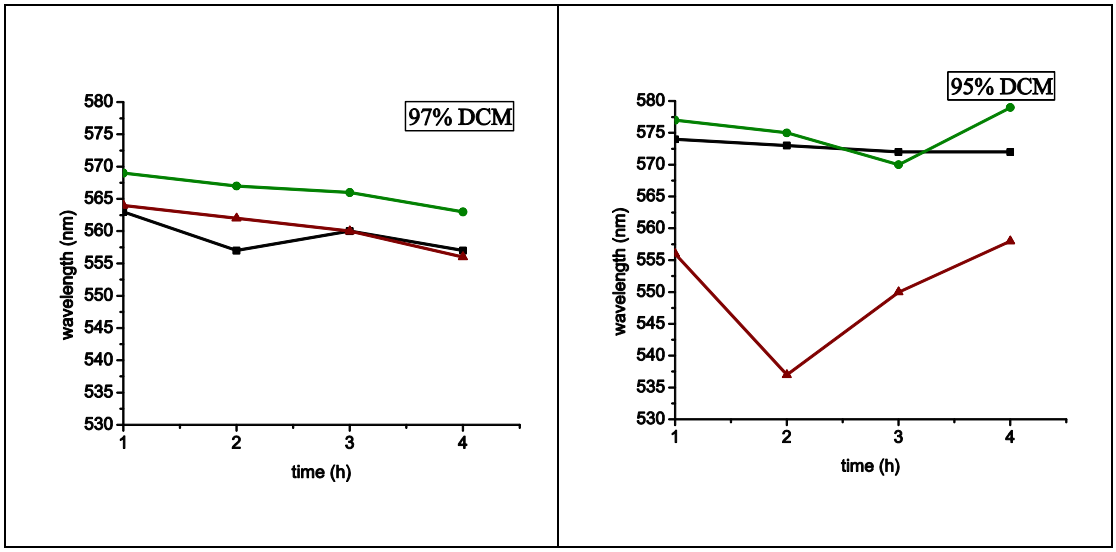

Figure 3.5: PL spectra of NBP3HT (black line), ROMPP3HT10 (green line), P3HT-PEO (brown line) in DCM-methanol (%DCM=v_{DCM} / [v_{DCM}+$v_{methanol}$] * 100%)

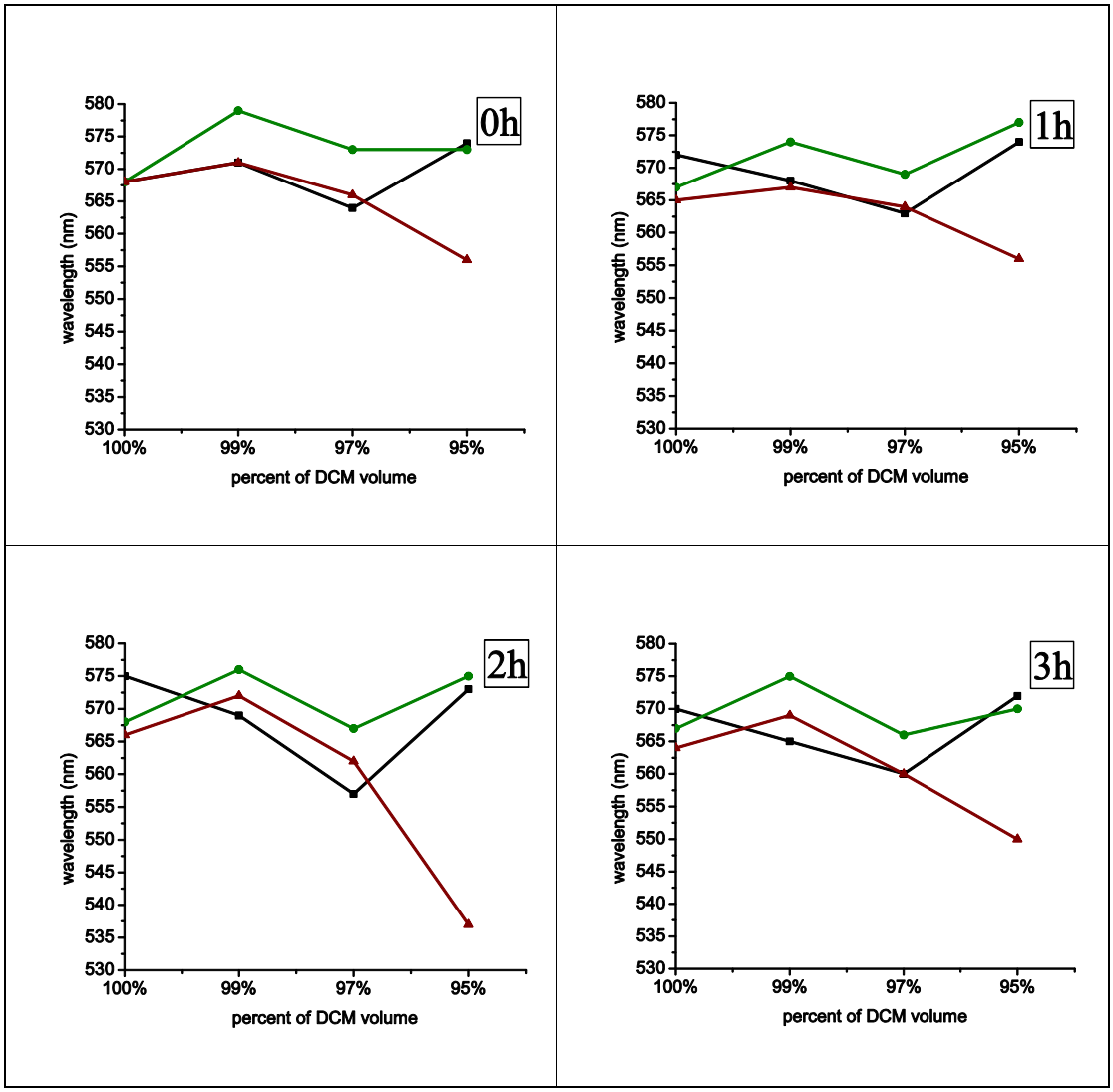

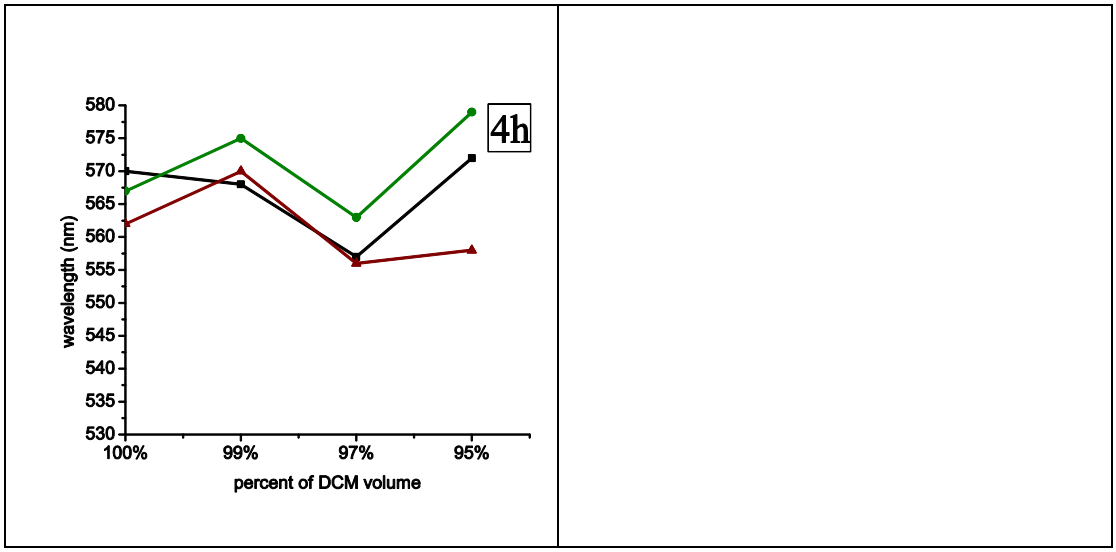

Figure 3.6: PL spectra of NBP3HT (black line), ROMPP3HT10 (green line), P3HT-PEO (brown line) in DCM－Methanol solution mixture by time

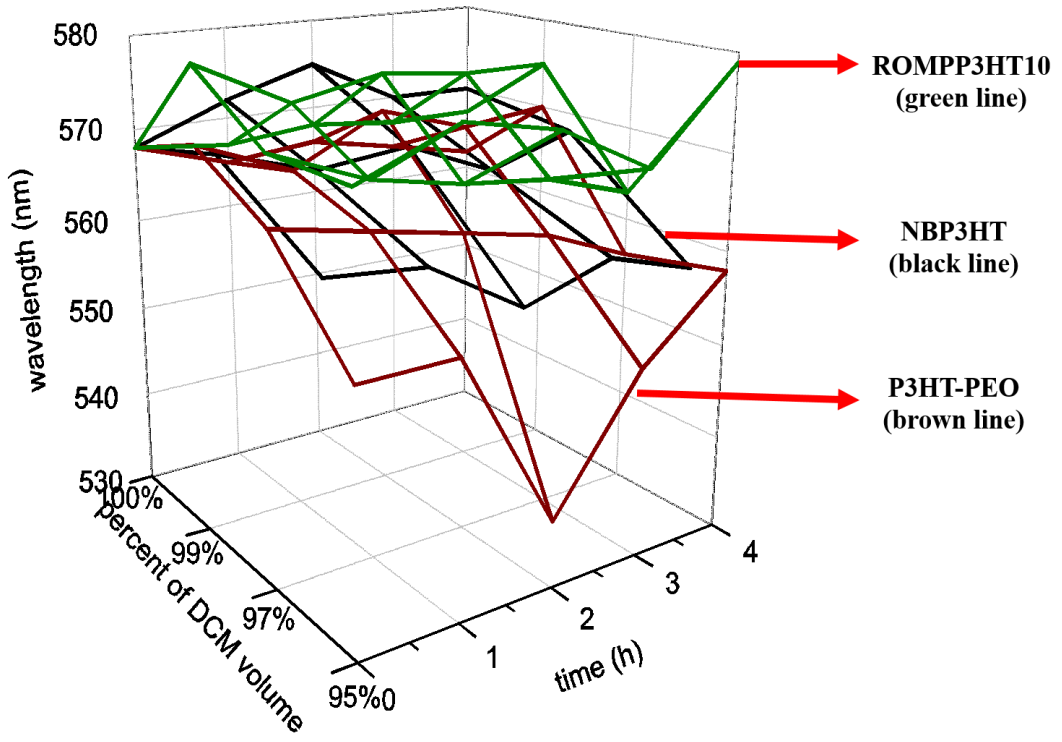

Figure 3.7 3D emission wavelength pattern for NBP3HT (black line), ROMPP3HT10 (green line), P3HT-PEO (brown line) in DCM－Methanol solution mixture with different time

Based on above observation, a continuous study was designed to further explore P3HT-PEO optical properties with smaller volume ratio of DCM. While P3HT-PEO start to precipitate when the volumetric ratio of methanol is more than 50% within 10min, a weak peak between 600nm-650nm was observed when in 50% DCM solution (Figure 3.8, Figure 3.9), indicating stable architectures were formed. The presence of this peak share similarity with linear P3HT-b-PEO, showing a transition coil form to aggregation form[41]. We assign the peak at around 580nm as 0-0 transition and peak at 620nm as 0-1 transition. When $I_{0\text{-}0}/I_{0\text{-}1}$ is over 1, it indicates intramolecular interaction dominate aggregation, makes the brush behave like linear copolymer. However, this architecture is not stable enough, as the time change, a 0-1 transition peak becomes weak and intensity of 0-0 peak becomes larger, showing an repulsive forces from brush itself may reorganize the aggregation of brush intramolecularly.

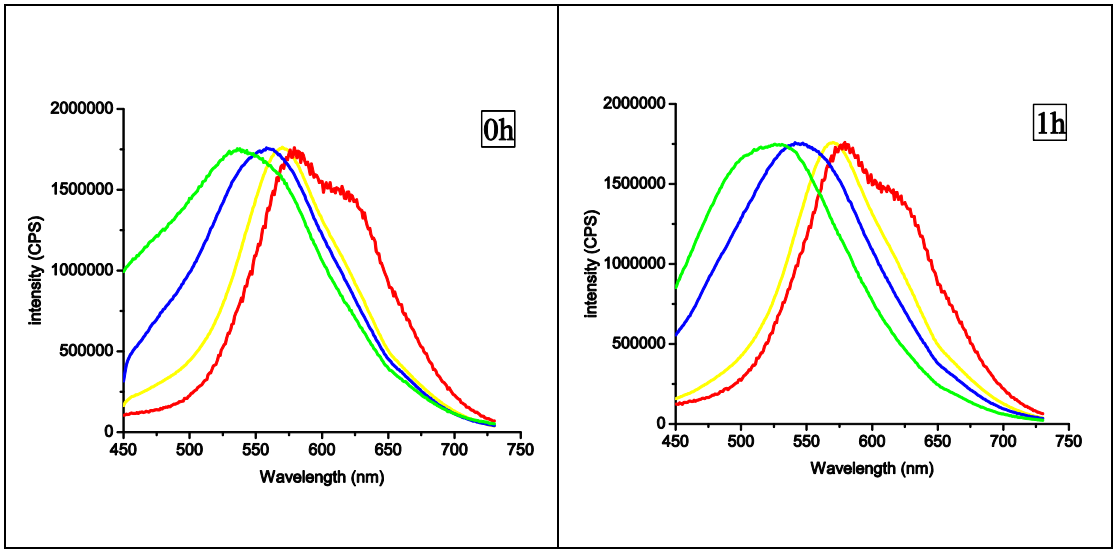

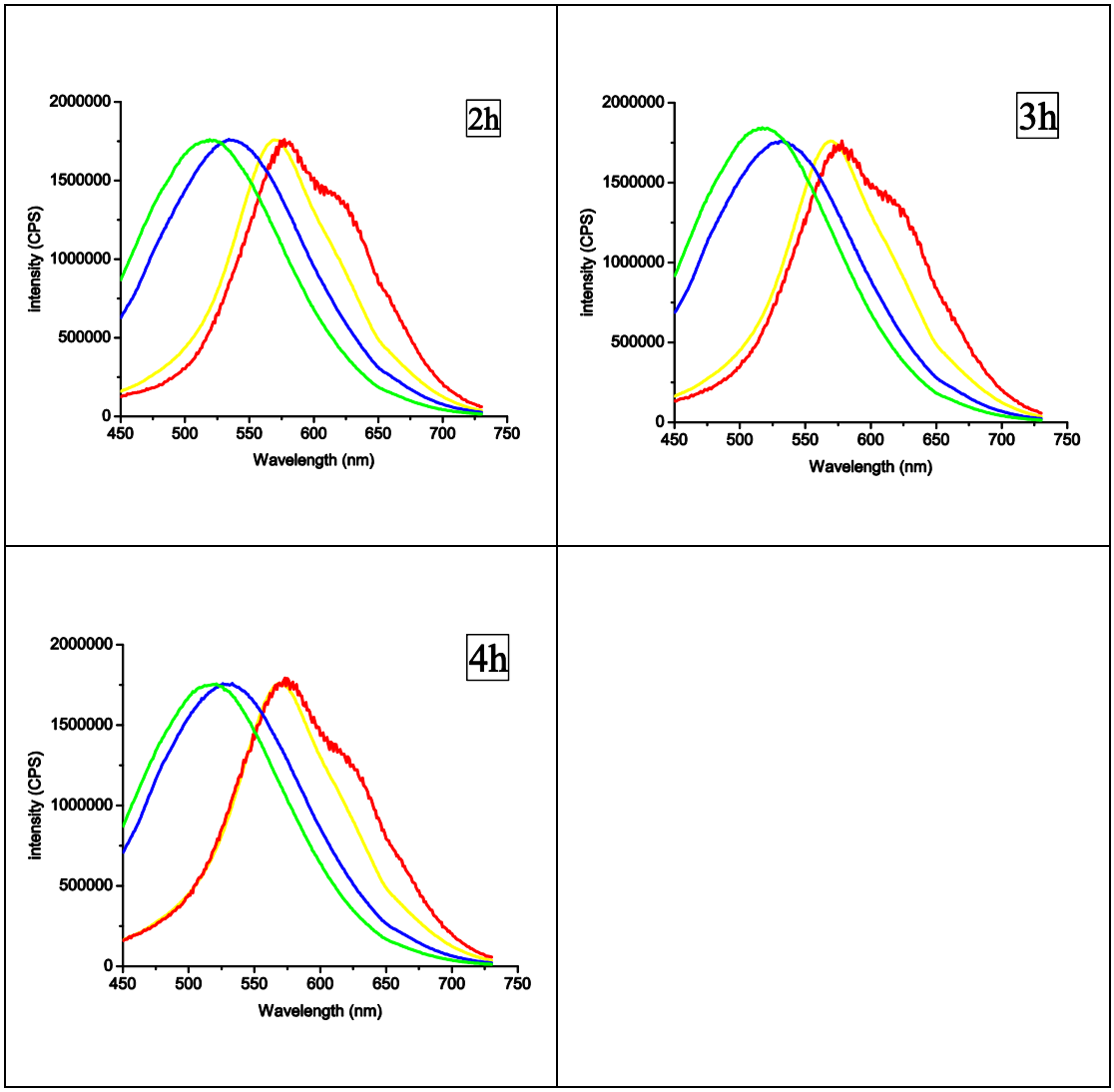

Figure 3.8: PL spectra of P3HT-PEO in DCM-methanol (v_{DCM}: $v_{methanol}$) mixture at different time (yellow line: 70% DCM; red line: 50% DCM; blue line: 30% DCM; green line: 10% DCM)

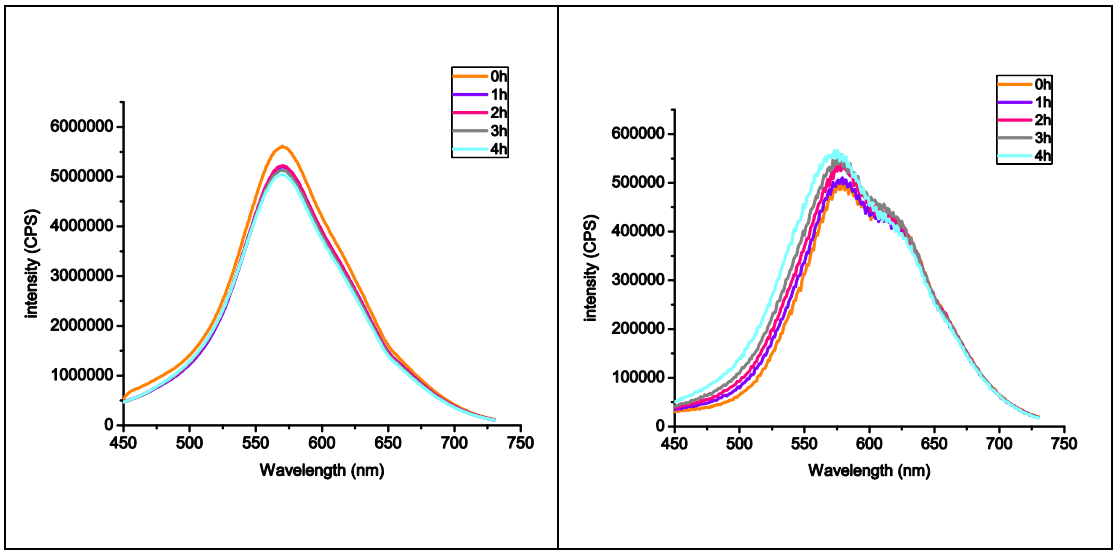

70% DCM	50% DCM
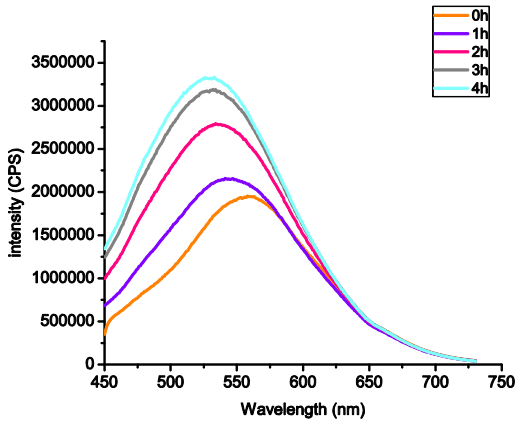	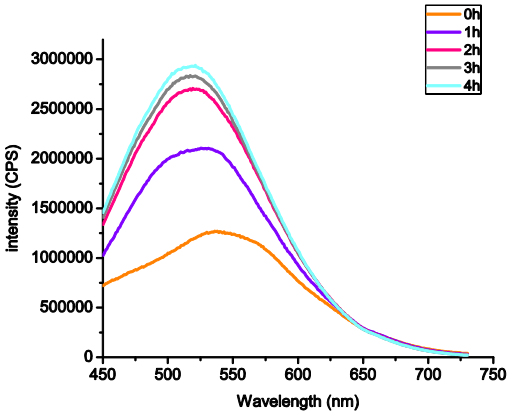
30% DCM	10% DCM

Figure 3.9: PL spectra of P3HT-PEO in DCM-methanol (v_{DCM}: $v_{methanol}$) mixture at different time

Even though precipitation was quickly formed when volume percentage DCM was smaller than 50%. It's interesting to find that blue shift was occurred (Figure 3.10) with increasing intensity, it may come from J favored aggregation at intramolecular level. Based on HJ-aggregation model[50], when P3HT-PEO is dissolved in solution, rearrangement of P3HT aggregation inside brush will occur.

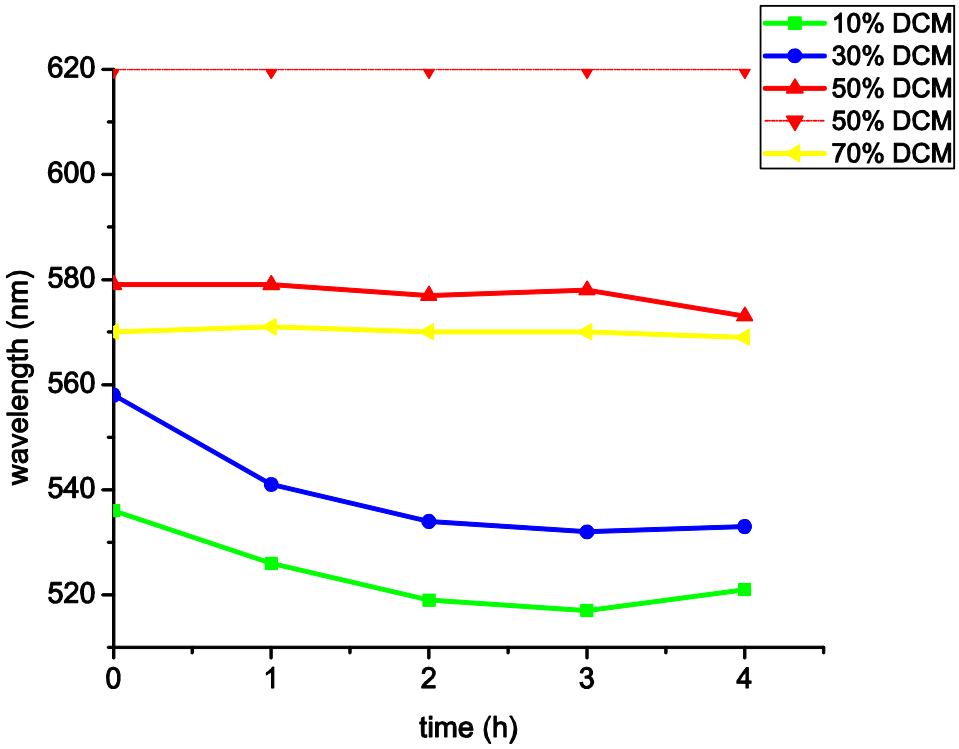

Figure 3.10: wavelength changes by time under different solution mixtures

3.3. Architectures of self-assembly from P3HT-PEO

All the polymer solution samples used in above fluorescence study is observed by Scanning Electron Microscopes (SEM) and Transmission Electron Microscopes (TEM) to figure out the structures. SEM samples were prepared by adding solutions onto clean glass substrates and the place to JEOL JSM-6335F after coating substrate. TEM samples were prepared by adding solution onto copper grid with carbon film, and then obtain structure information from JEOL JEM-2010 FasTEM.

Lamellar, nanofiber and micelle from linear P3HT copolymers are found as a result of crystalline forces[45,134,135,136]. NBP3HT can also be regarded as linear copolymer, therefore, the nanofiber structures formed from DCM solution can be explained (Figure

3.11).

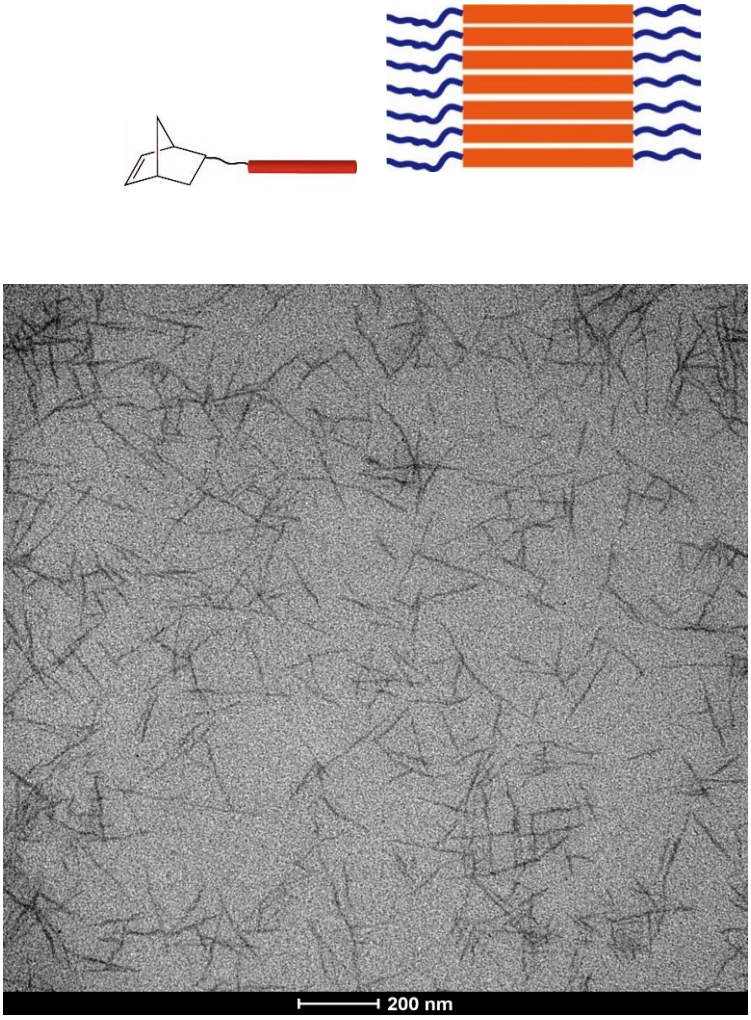

Figure 3.11: TEM of NBP3HT prepared by DCM solution

Cylindrical wormlike micelle were features of brush polymer as the repulsive side chain forces and semirigid backbone. In the solution, the forming of various structures of block copolymers are driven by 1) solvophilic/solvophobic force and 2) crystalline driven force. Semicrystalline P3HT is proved to form architectures mainly due to crystalline driving force[137,135, 138, 1], these may explain the probable architectures from P3HT-PEO: 1) micelle; and 2) nanorod (Figure 3.12)

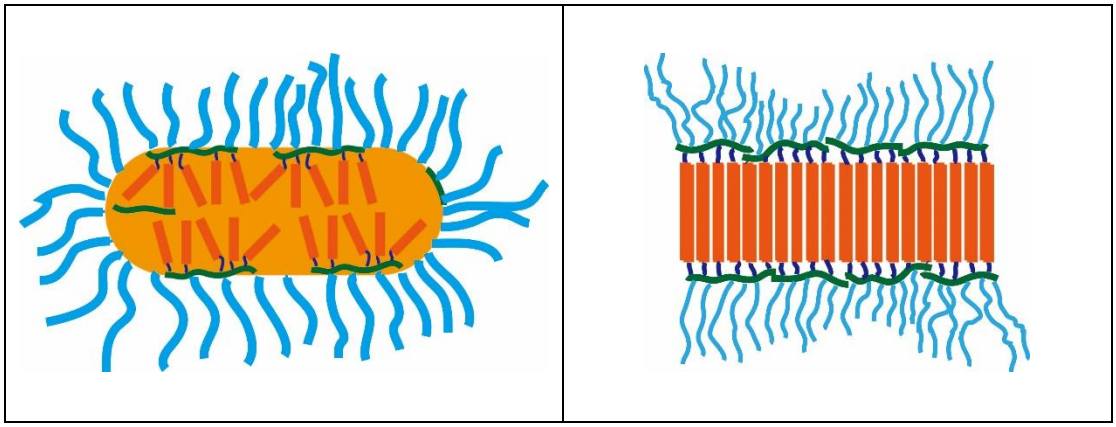

Figure 3.12: The formation of micelles and nanorod

However, neither these architectures were observed, instead, nanotubes were found. (Figure 3.13) This nanotube has features like: 1) it has a very clear contour line around the structure, like a shell around the tube, which is approximate 1/4 the width of the nanorod; 2) a hollow middle was formed in the middle of the rod, however, the middle resembles like bamboo or ladder; and 3) the length of rods are various.

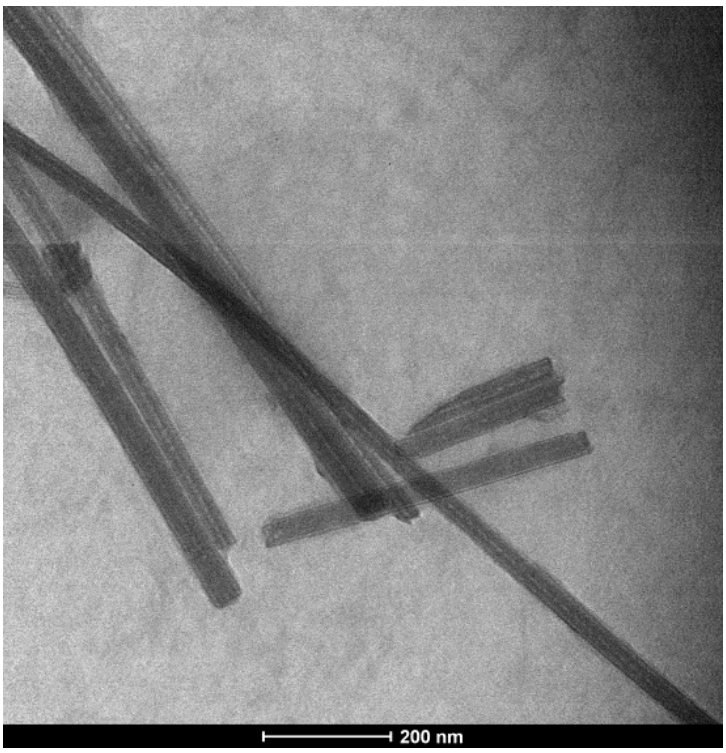

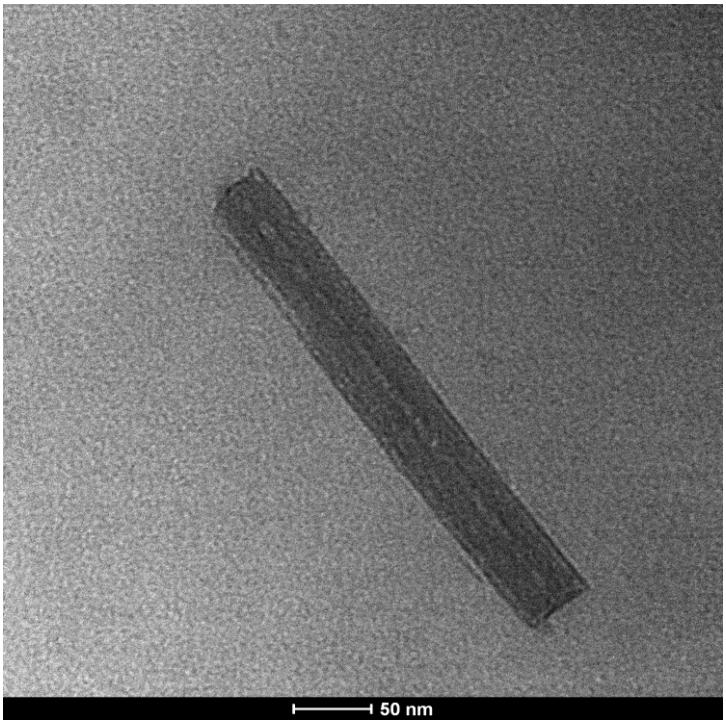

Figure 3.13 nanotubes from P3HT-PEO prepared by DCM-Methanol mixture (v_{DCM}: $v_{methanol}$=99:1)

Based on the aggregation study from linear P3HT-b-PEO, We proposed the formation of nanorods as following: nanorods are formed as the combination of π-π stacking and microphase separation; they are composed by two strips of nanowire; nanowires are formed by intermolecular interactions of P3HT aggregation (Figure 3.14a) first forms nanowire and at the same time microphase separation (Figure 3.14b) occurs to form lamellar architecture.

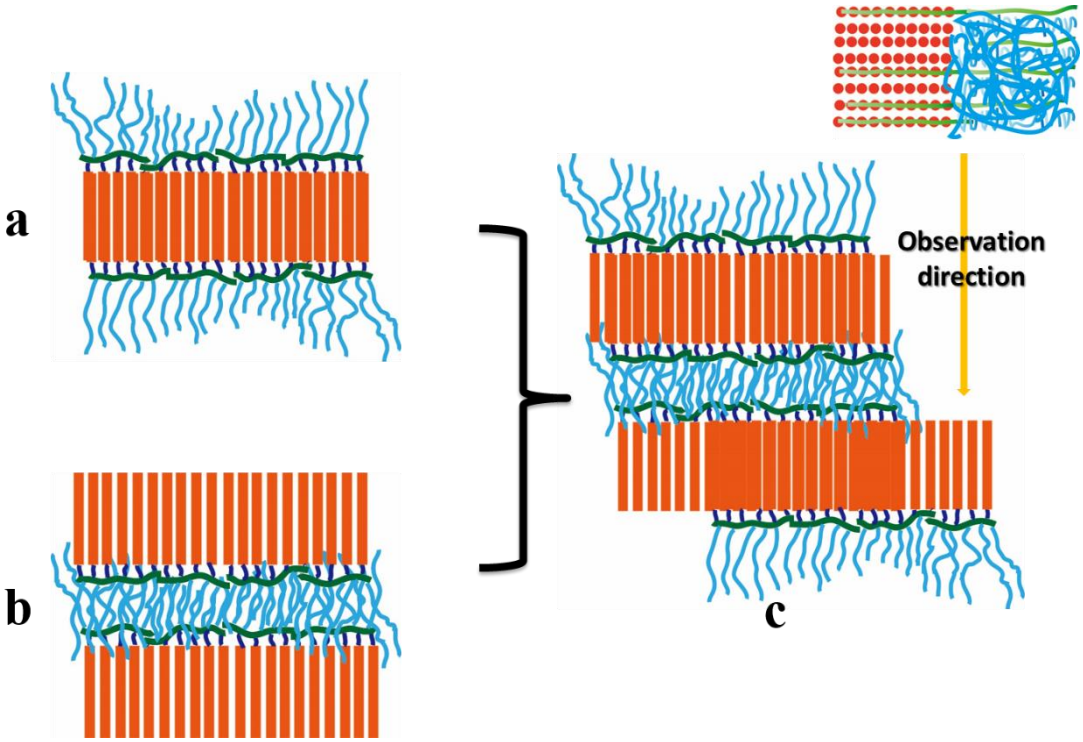

Figure 3.14: the formation of nanorod

4. CONCLUSION

We precisely synthesized well controlled dual brush polymer with determined Mw. However, degradation at low temperature occurred result in a failure to obtain nanostructures in solid state. Unique nanotube structure was observed from dual brush polymer which may result from a coeffect of aggregation and microphase separation. This may provide a new kind of conjugated material applicable to bioengineering.

5. REFERENCE

1. Yu, K.; Eisenberg, A., Multiple Morphologies in Aqueous Solutions of Aggregates of Polystyrene-block-poly(ethylene oxide) Diblock Copolymers. *Macromolecules* **1996,** *29* (19), 6359-6361.

2. Yu, K.; Eisenberg, A., Bilayer Morphologies of Self-Assembled Crew-Cut Aggregates of Amphiphilic PS-b-PEO Diblock Copolymers in Solution. *Macromolecules* **1998,** *31* (11), 3509-3518.

3. Zhu, L.; Cheng, S. Z. D.; Calhoun, B. H.; Ge, Q.; Quirk, R. P.; Thomas, E. L.; Hsiao, B. S.; Yeh, F.; Lotz, B., Phase structures and morphologies determined by self-organization, vitrification, and crystallization: confined crystallization in an ordered lamellar phase of PEO-b-PS diblock copolymer. *Polymer* **2001,** *42* (13), 5829-5839.

4. Khandpur, A. K.; Foerster, S.; Bates, F. S.; Hamley, I. W.; Ryan, A. J.; Bras, W.; Almdal, K.; Mortensen, K., Polyisoprene-Polystyrene Diblock Copolymer Phase Diagram near the Order-Disorder Transition. *Macromolecules* **1995,** *28* (26), 8796-8806.

5. Rzayev, J., Synthesis of Polystyrene−Polylactide Bottlebrush Block Copolymers and Their Melt Self-Assembly into Large Domain Nanostructures. *Macromolecules* **2009,** *42* (6), 2135-2141.

6. Choo, Y.; Mahajan, L. H.; Gopinadhan, M.; Ndaya, D.; Deshmukh, P.; Kasi, R. M.; Osuji, C. O., Phase Behavior of Polylactide-Based Liquid Crystalline Brushlike Block Copolymers. *Macromolecules* **2015,** *48* (22), 8315-8322.

7. Runge, M. B.; Bowden, N. B., Synthesis of High Molecular Weight Comb Block Copolymers and Their Assembly into Ordered Morphologies in the Solid State. *Journal of the American Chemical Society* **2007,** *129* (34), 10551-10560.

8. Han, D.; Tong, X.; Zhao, Y., One-Pot Synthesis of Brush Diblock Copolymers through Simultaneous ATRP and Click Coupling. *Macromolecules* **2011,** *44* (13), 5531-5536.

9. Lee, H.-i.; Matyjaszewski, K.; Yu-Su, S.; Sheiko, S. S., Hetero-Grafted Block Brushes with PCL and PBA Side Chains. *Macromolecules* **2008,** *41* (16), 6073-6080.

10. Fenyves, R.; Schmutz, M.; Horner, I. J.; Bright, F. V.; Rzayev, J., Aqueous Self-Assembly of Giant Bottlebrush Block Copolymer Surfactants as Shape-Tunable Building Blocks. *Journal of the American Chemical Society* **2014,** *136* (21), 7762-7770.

11. Yang, S.-H.; Lin, T.-S.; Huang, Y.-Z.; Li, H.-D.; Chao, Y.-C., Synthesis of hyperbranched polythiophenes containing tetrachloroperylene bisimide as bridging moiety for polymer solar cells. *Polymer* **2014,** *55* (23), 6058-6068.

12. (a) Zhou, E.; Tan, Z. a.; Yang, Y.; Huo, L.; Zou, Y.; Yang, C.; Li, Y., Synthesis, Hole Mobility, and Photovoltaic Properties of Cross-Linked Polythiophenes with Vinylene−Terthiophene−Vinylene as

Conjugated Bridge. *Macromolecules* **2007,** *40* (6), 1831-1837; (b) Hou, J.; Tan, Z. a.; Yan, Y.; He, Y.; Yang, C.; Li, Y., Synthesis and Photovoltaic Properties of Two-Dimensional Conjugated Polythiophenes with Bi(thienylenevinylene) Side Chains. *Journal of the American Chemical Society* **2006,** *128* (14), 4911-4916.

13. Małachowski, M. J.; Żmija, J., Organic field-effect transistors. *Opto-Electronics Review* **2010,** *18* (2), 121-136.

14. Nagapudi, K.; Brinkman, W. T.; Leisen, J.; Thomas, B. S.; Wright, E. R.; Haller, C.; Wu, X.; Apkarian, R. P.; Conticello, V. P.; Chaikof, E. L., Protein-Based Thermoplastic Elastomers. *Macromolecules* **2005,** *38* (2), 345-354.

15. Nowak, A. P.; Breedveld, V.; Pakstis, L.; Ozbas, B.; Pine, D. J.; Pochan, D.; Deming, T. J., Rapidly recovering hydrogel scaffolds from self-assembling diblock copolypeptide amphiphiles. *Nature* **2002,** *417* (6887), 424-428.

16. Fu, Q.; Livengood, B. P.; Shen, C. C.; Lin, F. L.; Harris, F. W.; Cheng, S. Z. D.; Hsiao, B. S.; Yeh, F., Crystallization and phase behavior in nylon 6/aromatic polyimide triblock copolymers. *Macromolecular Chemistry and Physics* **1998,** *199* (6), 1107-1118.

17. Takayanagi, M.; Ogata, T.; Morikawa, M.; Kai, T., Polymer composites of rigid and flexible molecules: System of wholly aromatic and aliphatic polyamides. *Journal of Macromolecular Science, Part B* **1980,** *17* (4), 591-615.

18. Cornelissen, J. J. L. M.; Fischer, M.; Sommerdijk, N. A. J. M.; Nolte, R. J. M., Helical superstructures from charged poly(styrene)- poly(isocyanodipeptide) block copolymers. *Science* **1998,** *280* (5368), 1427-1430.

19. Cai, C.; Lin, J.; Chen, T.; Wang, X.-S.; Lin, S., Super-helices self-assembled from a binary system of amphiphilic polypeptide block copolymers and polypeptide homopolymers. *Chemical Communications* **2009,** (19), 2709-2711.

20. Zubarev, E. R.; Pralle, M. U.; Sone, E. D.; Stupp, S. I., Self-Assembly of Dendron Rodcoil Molecules into Nanoribbons. *Journal of the American Chemical Society* **2001,** *123* (17), 4105-4106.

21. Lee, E.; Kim, J.-K.; Lee, M., Tubular Stacking of Water-Soluble Toroids Triggered by Guest Encapsulation. *Journal of the American Chemical Society* **2009,** *131* (51), 18242-18243.

22. Liu, L.; Kim, J.-K.; Lee, M., Mesoscale Surface Patterning of a Laterally-Grafted Rod Amphiphile: Rings And Fibers. *ChemPhysChem* **2010,** *11* (3), 706-712.

23. Park, I.-S.; Yoon, Y.-R.; Jung, M.; Kim, K.; Park, S.; Shin, S.; Lim, Y.-b.; Lee, M., Designer Nanorings with Functional Cavities from Self-Assembling β-Sheet Peptides. *Chemistry – An Asian Journal* **2011,** *6* (2), 452-458.

24. Tenneti, K. K.; Chen, X.; Li, C. Y.; Tu, Y.; Wan, X.; Zhou, Q.-F.; Sics, I.; Hsiao, B. S., Perforated Layer Structures in Liquid Crystalline Rod−Coil Block Copolymers. *Journal of the American Chemical Society* **2005,** *127* (44), 15481-15490.

25. Chen, J. T.; Thomas, E. L.; Ober, C. K.; Hwang, S. S., Zigzag morphology of a poly(styrene-b-hexyl isocyanate) rod-coil block copolymer. *Macromolecules* **1995,** *28* (5), 1688-1697.

26. Pryamitsyn, V.; Ganesan, V., Self-assembly of rod–coil block copolymers. *The Journal of Chemical Physics* **2004,** *120* (12), 5824-5838.

27. Zhang, J.; Yu, Z.; Wan, X.; Chen, X.; Zhou, Q., Synthesis and Characterization of Helix-Coil Diblock Copolymers with Controlled Supramolecular Architectures in Aqueous Solution. *Macromolecular Rapid Communications* **2005,** *26* (15), 1241-1245.

28. Kim, H.-J.; Kang, S.-K.; Lee, Y.-K.; Seok, C.; Lee, J.-K.; Zin, W.-C.; Lee, M., Self-Dissociating Tubules from Helical Stacking of Noncovalent Macrocycles. *Angewandte Chemie International Edition* **2010,** *49* (45), 8471-8475.

29. McQuade, D. T.; Pullen, A. E.; Swager, T. M., Conjugated Polymer-Based Chemical Sensors. *Chemical Reviews* **2000,** *100* (7), 2537-2574.

30. Zhou, C. Y.; Yan, L. T.; Zhang, L. N.; Ai, X. D.; Li, T. X.; Dai, C. A., Synthesis of Regioregular 3-carboxylic Ester-substituted Polythiophene and its Copolymer with Thiophene. *Journal of Macromolecular Science: Pure & Applied Chemistry* **2012,** *49* (4), 293-297.

31. Kovacik, P.; Willis, S. M.; Matichak, J. D.; Assender, H. E.; Watt, A. A. R., Effect of side groups on the vacuum thermal evaporation of polythiophenes for organic electronics. *Organic Electronics* **2012,** *13* (4), 687-696.

32. Shang, H.; Fan, H.; Liu, Y.; Hu, W.; Li, Y.; Zhan, X., New X-shaped oligothiophenes for solution-processed solar cells. *Journal of Materials Chemistry* **2011,** *21* (26), 9667-9673.

33. Kuila, B. K.; Park, K.; Dai, L., Soluble P3HT-Grafted Carbon Nanotubes: Synthesis and Photovoltaic Application. *Macromolecules* **2010,** *43* (16), 6699-6705.

34. Osaka, I.; McCullough, R. D., Advances in molecular design and synthesis of regioregular polythiophenes. *Accounts of Chemical Research* **2008,** *41* (9), 1202-1214.

35. Liu, C.-L.; Lin, C.-H.; Kuo, C.-C.; Lin, S.-T.; Chen, W.-C., Conjugated rod–coil block copolymers: Synthesis, morphology, photophysical properties, and stimuli-responsive applications. *Progress in Polymer Science* **2011,** *36* (5), 603-637.

36. Su, M.; Shi, S.-Y.; Wang, Q.; Liu, N.; Yin, J.; Liu, C.; Ding, Y.; Wu, Z.-Q., Multi-responsive behavior of highly water-soluble poly(3-hexylthiophene)-block-poly(phenyl isocyanide) block copolymers.

Polymer Chemistry **2015,** *6* (36), 6519-6528.

37. Roncali, J., Conjugated poly(thiophenes): Synthesis, functionalization, and applications. *Chemical Reviews* **1992,** *92* (4), 711-738.

38. Lee, J. U.; Jung, J. W.; Emrick, T.; Russell, T. P.; Jo, W. H., Synthesis of C60-end capped P3HT and its application for high performance of P3HT/PCBM bulk heterojunction solar cells. *Journal of Materials Chemistry* **2010,** *20* (16), 3287-3294.

39. Zehm, D.; Laschewsky, A.; Gradzielski, M.; Prévost, S.; Liang, H.; Rabe, J. P.; Schweins, R.; Gummel, J., Amphiphilic Dual Brush Block Copolymers as "Giant Surfactants" and Their Aqueous Self-Assembly. *Langmuir* **2010,** *26* (5), 3145-3155.

40. Lanzi, M.; Di-Nicola, F. P.; Errani, F.; Paganin, L.; Mucci, A., Solventless deposition of oligo- and polythiophenes for bulk heterojunction solar cells. *Synthetic Metals* **2014,** *195* (0), 61-68.

41. He, L.; Pan, S.; Peng, J., Morphology control of poly(3-hexylthiophene)-b-poly(ethylene oxide) block copolymer by solvent blending. *Journal of Polymer Science Part B: Polymer Physics* **2016,** *54* (5), 544-551.

42. Murphy, A. R.; Liu, J.; Luscombe, C.; Kavulak, D.; Fréchet, J. M. J.; Kline, R. J.; McGehee, M. D., Synthesis, Characterization, and Field-Effect Transistor Performance of Carboxylate-Functionalized Polythiophenes with Increased Air Stability. *Chemistry of Materials* **2005,** *17* (20), 4892-4899.

43. Qu, B.; Jiang, Z.; Chen, Z.; Xiao, L.; Tian, D.; Gao, C.; Wei, W.; Gong, Q., Synthesis of a soluble polythiophene copolymer with thiophene–vinylene conjugated side chain and its applications in photovoltaic devices. *Journal of Applied Polymer Science* **2012,** *124* (2), 1186-1192.

44. Boudouris, B. W.; Frisbie, C. D.; Hillmyer, M. A., Nanoporous poly(3-alkylthiophene) thin films generated from block copolymer templates. *Macromolecules* **2008,** *41* (1), 67-75.

45. Kamps, A. C.; Fryd, M.; Park, S.-J., Hierarchical self-assembly of amphiphilic semiconducting polymers into isolated, bundled, and branched nanofibers.pdf. *ACS Nano* **2012,** *6* (3), 2844-2852.

46. Lu, K.; Guo, Y.; Liu, Y.; Di, C.-a.; Li, T.; Wei, Z.; Yu, G.; Du, C.; Ye, S., Novel Functionalized Conjugated Polythiophene with Oxetane Substituents: Synthesis, Optical, Electrochemical, and Field-Effect Properties. *Macromolecules* **2009,** *42* (9), 3222-3226.

47. Dai, C. A.; Yen, W. C.; Lee, Y. H.; Ho, C. C.; Su, W. F., Facile synthesis of well-defined block copolymers containing regioregular poly(3-hexyl thiophene) via anionic macroinitiation method and their self-assembly behavior. *Journal of the American Chemical Society* **2007,** *129* (36), 11036-11038.

48. Ho, V.; Boudouris, B. W.; McCulloch, B. L.; Shuttle, C. G.; Burkhardt, M.; Chabinyc, M. L.; Segalman, R. A., Poly(3-alkylthiophene) diblock copolymers with ordered microstructures and

continuous semiconducting pathways. *Journal of the American Chemical Society* **2011,** *133* (24), 9270-9273.

49. Zhang, M.; Guo, X.; Yang, Y.; Zhang, J.; Zhang, Z.-G.; Li, Y., Downwards tuning the HOMO level of polythiophene by carboxylate substitution for high open-circuit-voltage polymer solar cells. *Polymer Chemistry* **2011,** *2* (12), 2900-2906.

50. Spano, F. C.; Silva, C., H- and J-Aggregate Behavior in Polymeric Semiconductors. *Annual Review of Physical Chemistry* **2014,** *65* (1), 477-500.

51. Spano, F. C., Modeling disorder in polymer aggregates: The optical spectroscopy of regioregular poly(3-hexylthiophene) thin films. *The Journal of Chemical Physics* **2005,** *122* (23), 234701.

52. Clark, J.; Silva, C.; Friend, R. H.; Spano, F. C., Role of Intermolecular Coupling in the Photophysics of Disordered Organic Semiconductors: Aggregate Emission in Regioregular Polythiophene. *Physical Review Letters* **2007,** *98* (20), 206406.

53. Clark, J.; Chang, J.-F.; Spano, F. C.; Friend, R. H.; Silva, C., Determining exciton bandwidth and film microstructure in polythiophene films using linear absorption spectroscopy. *Applied Physics Letters* **2009,** *94* (16), 163306.

54. Niles, E. T.; Roehling, J. D.; Yamagata, H.; Wise, A. J.; Spano, F. C.; Moulé, A. J.; Grey, J. K., J-Aggregate Behavior in Poly-3-hexylthiophene Nanofibers. *The Journal of Physical Chemistry Letters* **2012,** *3* (2), 259-263.

55. Fleischli, F. D.; Ghasdian, N.; Georgiou, T. K.; Stingelin, N., Tailoring the optical properties of poly(3-hexylthiophene) by emulsion processing using polymeric macrosurfactants. *Journal of Materials Chemistry C* **2015,** *3* (9), 2065-2071.

56. Hu, Z.; Adachi, T.; Haws, R.; Shuang, B.; Ono, R. J.; Bielawski, C. W.; Landes, C. F.; Rossky, P. J.; Vanden Bout, D. A., Excitonic Energy Migration in Conjugated Polymers: The Critical Role of Interchain Morphology. *Journal of the American Chemical Society* **2014,** *136* (45), 16023-16031.

57. Gao, J.; Kamps, A.; Park, S.-J.; Grey, J. K., Encapsulation of Poly(3-hexylthiophene) J-Aggregate Nanofibers with an Amphiphilic Block Copolymer. *Langmuir* **2012,** *28* (47), 16401-16407.

58. Baghgar, M.; Pentzer, E.; Wise, A. J.; Labastide, J. A.; Emrick, T.; Barnes, M. D., Cross-Linked Functionalized Poly(3-hexylthiophene) Nanofibers with Tunable Excitonic Coupling. *ACS Nano* **2013,** *7* (10), 8917-8923.

59. Willot, P.; Moerman, D.; Leclère, P.; Lazzaroni, R.; Baeten, Y.; Van der Auweraer, M.; Koeckelberghs, G., One-Pot Synthesis and Characterization of All-Conjugated Poly(3-alkylthiophene)-block-poly(dialkylthieno[3,4-b]pyrazine). *Macromolecules* **2014,** *47* (19), 6671-6678.

60. Pang, X.; Zhao, L.; Feng, C.; Lin, Z., Novel amphiphilic multiarm, starlike coil-rod diblock copolymers via a combination of click chemistry with living polymerization. *Macromolecules* **2011,** *44* (18), 7176-7183.

61. Mohamed, M. G.; Cheng, C.-C.; Lin, Y.-C.; Huang, C.-W.; Lu, F.-H.; Chang, F.-C.; Kuo, S.-W., Synthesis and self-assembly of water-soluble polythiophene-graft-poly(ethylene oxide) copolymers. *RSC Advances* **2014,** *4* (42), 21830-21839.

62. Sivula, K. a.; Ball, Z. T. b.; Watanabe, N. b.; Fréchet, J. M. J., Amphiphilic diblock copolymer compatibilizers and their effect on the morphology and performance of polythiophene Fullerene solar cells-supporting information.pdf. *Advanced Materials* **2006,** *18* (2), 206.

63. Yun, M. H.; Kim, J.; Yang, C.; Kim, J. Y., A simultaneous achievement of high performance and extended thermal stability of bulk-heterojunction polymer solar cells using a polythiophene–fullerene block copolymer. *Solar Energy Materials and Solar Cells* **2012,** *104* (0), 7-12.

64. Wang, Y.; Zhou, E.; Liu, Y.; Xi, H.; Ye, S.; Wu, W.; Guo, Y.; Di, C.-a.; Sun, Y.; Yu, G.; Li, Y., Solution-Processed Organic Field-Effect Transistors Based on Polythiophene Derivatives with Conjugated Bridges as Linking Chains. *Chemistry of Materials* **2007,** *19* (14), 3361-3363.

65. Meng, K.; Ding, Q.; Wang, S.; He, Y.; Li, Y.; Gong, Q., Spatial Conformation and Charge Recombination Properties of Polythiophene Deriatives with Thienylene−Vinylene Side Chains Investigated by Static and Femtosecond Spectroscopy. *The Journal of Physical Chemistry B* **2010,** *114* (8), 2602-2606.

66. Hilf, S.; Klos, J.; Char, K.; Woo, H.; Kilbinger, A. F. M., Polymerizable well-defined oligo(thiophene amide)s and their ROMP block copolymers. *Macromolecular Rapid Communications* **2009,** *30* (14), 1249-1257.

67. Pang, X.; Zhao, L.; Feng, C.; Wu, R.; Ma, H.; Lin, Z., Functional copolymer brushes composed of a hydrophobic backbone and densely grafted conjugated side chains via a combination of living polymerization with click chemistry. *Polymer Chemistry* **2013,** *4* (6), 2025-2032.

68. Ahn, S. K.; Pickel, D. L.; Kochemba, W. M.; Chen, J.; Uhrig, D.; Hinestrosa, J. P.; Carrillo, J. M.; Shao, M.; Do, C.; Messman, J. M.; Brown, W. M.; Sumpter, B. G.; Kilbey, S. M., Poly(3-hexylthiophene) molecular bottlebrushes via ring-opening metathesis polymerization: Macromolecular architecture enhanced aggregation. *ACS Macro Letters* **2013,** *2* (8), 761-765.

69. van As, D.; Subbiah, J.; Jones, D. J.; Wong, W. W. H., Controlled Synthesis of Well-Defined Semiconducting Brush Polymers. *Macromolecular Chemistry and Physics* **2016,** *217* (3), 403-413.

70. Hayakawa, T.; Horiuchi, S., From angstroms to micrometers: Self-organized hierarchical structure within a polymer film. *Angewandte Chemie - International Edition* **2003,** *42* (20), 2285-2289.

71. Qiao, Y.; Islam, M. S.; Yin, X.; Han, K.; Yan, Y.; Zhang, J.; Wang, Q.; Ploehn, H. J.; Tang, C., Oligothiophene-containing polymer brushes by ROMP and RAFT: Synthesis, characterization and dielectric properties. *Polymer* **2015,** *72*, 428-435.

72. Pryamitsyn, V.; Ganesan, V., Self-assembly of rod-coil block copolymers. *Journal of Chemical Physics* **2004,** *120* (12), 5824-5838.

73. Tenneti, K. K.; Chen, X.; Li, C. Y.; Tu, Y.; Wan, X.; Zhou, Q. F.; Sics, I.; Hsiao, B. S., Perforated layer structures in liquid crystalline rod-coil block copolymers. *Journal of the American Chemical Society* **2005,** *127* (44), 15481-15490.

74. Olsen, B. D.; Segalman, R. A., Structure and thermodynamics of weakly segregated rod-coil block copolymers. *Macromolecules* **2005,** *38* (24), 10127-10137.

75. Sumerlin, B. S.; Neugebauer, D.; Matyjaszewski, K., Initiation Efficiency in the Synthesis of Molecular Brushes by Grafting from via Atom Transfer Radical Polymerization. *Macromolecules* **2005,** *38* (3), 702-708.

76. Cheng, C.; Qi, K.; Khoshdel, E.; Wooley, K. L., Tandem Synthesis of Core−Shell Brush Copolymers and Their Transformation to Peripherally Cross-Linked and Hollowed Nanostructures. *Journal of the American Chemical Society* **2006,** *128* (21), 6808-6809.

77. Gao, H.; Matyjaszewski, K., Synthesis of Molecular Brushes by "Grafting onto" Method: Combination of ATRP and Click Reactions. *Journal of the American Chemical Society* **2007,** *129* (20), 6633-6639.

78. Muehlebach, A.; Rime, F., Synthesis of well-defined macromonomers and comb copolymers from polymers made by atom transfer radical polymerization. *Journal of Polymer Science Part A: Polymer Chemistry* **2003,** *41* (21), 3425-3439.

79. Durmaz, H.; Dag, A.; Cerit, N.; Sirkecioglu, O.; Hizal, G.; Tunca, U., Graft copolymers via ROMP and Diels–Alder click reaction strategy. *Journal of Polymer Science Part A: Polymer Chemistry* **2010,** *48* (24), 5982-5991.

80. Le, D.; Montembault, V.; Soutif, J. C.; Rutnakornpituk, M.; Fontaine, L., Synthesis of Well-Defined ω-Oxanorbornenyl Poly(ethylene oxide) Macromonomers via Click Chemistry and Their Ring-Opening Metathesis Polymerization. *Macromolecules* **2010,** *43* (13), 5611-5617.

81. Bielawski, C. W.; Grubbs, R. H., Living ring-opening metathesis polymerization. *Progress in Polymer Science* **2007,** *32* (1), 1-29.

82. Deshmukh, P.; Gopinadhan, M.; Choo, Y.; Ahn, S.-k.; Majewski, P. W.; Yoon, S. Y.; Bakajin, O.; Elimelech, M.; Osuji, C. O.; Kasi, R. M., Molecular Design of Liquid Crystalline Brush-Like Block Copolymers for Magnetic Field Directed Self-Assembly: A Platform for Functional Materials. *ACS Macro*

Letters **2014,** *3* (5), 462-466.

83. Dag, A.; Sahin, H.; Durmaz, H.; Hizal, G.; Tunca, U., Block-brush copolymers via ROMP and sequential double click reaction strategy. *Journal of Polymer Science Part A: Polymer Chemistry* **2011,** *49* (4), 886-892.

84. Cheng, C.; Khoshdel, E.; Wooley, K. L., ATRP from a Norbornenyl-Functionalized Initiator: Balancing of Complementary Reactivity for the Preparation of α-Norbornenyl Macromonomers/ω-Haloalkyl Macroinitiators. *Macromolecules* **2005,** *38* (23), 9455-9465.

85. Morandi, G.; Piogé, S.; Pascual, S.; Montembault, V.; Legoupy, S.; Fontaine, L., ATRP and ROMP: Modular chemical tools for advanced macromolecular engineering. *Materials Science and Engineering: C* **2009,** *29* (2), 367-371.

86. Cheng, C.; Khoshdel, E.; Wooley, K. L., Facile one-pot synthesis of brush polymers through tandem catalysis using Grubbs' catalyst for both ring-opening metathesis and atom transfer radical polymerizations. *Nano Letters* **2006,** *6* (8), 1741-1746.

87. Rizmi, A. C. M.; Khosravi, E.; Feast, W. J.; Mohsin, M. A.; Johnson, A. F., Synthesis of well-defined graft copolymers via coupled living anionic polymerization and living ROMP. *Polymer* **1998,** *39* (25), 6605-6610.

88. Cheng, C.; Yang, N. L., Well-defined diblock macromonomer with a norbornene group at block junction: Anionic living linking synthesis and ring-opening metathesis polymerization. *Macromolecules* **2010,** *43* (7), 3153-3155.

89. Khosravi, E.; Hutchings, L. R.; Kujawa-Welten, M., Synthesis of well-defined graft co-polymers via coupled living anionic and living ring-opening metathesis polymerisation. *Designed Monomers and Polymers* **2004,** *7* (6), 619-632.

90. Sukegawa, T.; Masuko, I.; Oyaizu, K.; Nishide, H., Expanding the Dimensionality of Polymers Populated with Organic Robust Radicals toward Flow Cell Application: Synthesis of TEMPO-Crowded Bottlebrush Polymers Using Anionic Polymerization and ROMP. *Macromolecules* **2014,** *47* (24), 8611-8617.

91. Li, Z.; Zhang, K.; Ma, J.; Cheng, C.; Wooley, K. L., Facile syntheses of cylindrical molecular brushes by a sequential RAFT and ROMP “grafting-through” methodology. *Journal of Polymer Science Part A: Polymer Chemistry* **2009,** *47* (20), 5557-5563.

92. Cheng, C.; Khoshdel, E.; Wooley, K. L., One-pot tandem synthesis of a core-shell brush copolymer from small molecule reactants by ring-opening metathesis and reversible addition-fragmentation chain transfer (co)polymerizations. *Macromolecules* **2007,** *40* (7), 2289-2292.

93. Kolb, H. C.; Finn, M. G.; Sharpless, K. B., Click Chemistry: Diverse Chemical Function from a

Few Good Reactions. *Angewandte Chemie International Edition* **2001,** *40* (11), 2004-2021.

94. Xia, Y.; Kornfield, J. A.; Grubbs, R. H., Efficient Synthesis of Narrowly Dispersed Brush Polymers via Living Ring-Opening Metathesis Polymerization of Macromonomers. *Macromolecules* **2009,** *42* (11), 3761-3766.

95. Le, D.; Morandi, G.; Legoupy, S.; Pascual, S.; Montembault, V.; Fontaine, L., Cyclobutenyl macromonomers: Synthetic strategies and ring-opening metathesis polymerization. *European Polymer Journal* **2013,** *49* (5), 972-983.

96. Le, D.; Montembault, V.; Pascual, S.; Legoupy, S.; Fontaine, L., An Orthogonal Modular Approach to Macromonomers Using Clickable Cyclobutenyl Derivatives and RAFT Polymerization. *Macromolecules* **2012,** *45* (19), 7758-7769.

97. Le, D.; Montembault, V.; Pascual, S.; Collette, F.; Heroguez, V.; Fontaine, L., Synthesis of 1,4-polybutadiene-g-poly(ethylene oxide) via the macromonomer approach by ROMP. *Polymer Chemistry* **2013,** *4* (6), 2168-2173.

98. Xia, Y.; Olsen, B. D.; Kornfield, J. A.; Grubbs, R. H., Efficient synthesis of narrowly dispersed brush copolymers and study of their assemblies: The importance of side chain arrangement. *Journal of the American Chemical Society* **2009,** *131* (51), 18525-18532.

99. Jeffries-El, M.; Sauvé, G.; McCullough, R. D., Facile synthesis of end-functionalized regioregular poly(3-alkylthiophene)s via modified Grignard metathesis reaction.pdf. *Macromolecules* **2005,** *38* (25), 10346-10352.

100. Iovu, M. C.; Jeffries-El, M.; Sheina, E. E.; Cooper, J. R.; McCullough, R. D., Regioregular poly(3-alkylthiophene) conducting block copolymers. *Polymer* **2005,** *46* (19), 8582-8586.

101. Iovu, M. C.; Zhang, R.; Cooper, J. R.; Smilgies, D. M.; Javier, A. E.; Sheina, E. E.; Kowalewski, T.; McCullough, R. D., Conducting block copolymers of regioregular poly(3-hexylthiophene) and poly(methacrylates): Electronic materials with variable conductivities and degrees of interfibrillar order. *Macromolecular Rapid Communications* **2007,** *28* (17), 1816-1824.

102. Huo, L.; Zhou, Y.; Li, Y., Alkylthio-Substituted Polythiophene: Absorption and Photovoltaic Properties. *Macromolecular Rapid Communications* **2009,** *30* (11), 925-931.

103. Prosa, T. J.; Winokur, M. J.; McCullough, R. D., Evidence of a Novel Side Chain Structure in Regioregular Poly(3-alkylthiophenes). *Macromolecules* **1996,** *29* (10), 3654-3656.

104. Klärner, G.; Lee, J. I.; Lee, V. Y.; Chan, E.; Chen, J. P.; Nelson, A.; Markiewicz, D.; Siemens, R.; Scott, J. C.; Miller, R. D., Cross-linkable Polymers Based on Dialkylfluorenes. *Chemistry of Materials* **1999,** *11* (7), 1800-1805.

105. Cheng, G.; Böker, A.; Zhang, M.; Krausch, G.; Müller, A. H. E., Amphiphilic Cylindrical Core−Shell Brushes via a "Grafting From" Process Using ATRP. *Macromolecules* **2001,** *34* (20), 6883-6888.

106. Lee, H.-i.; Jakubowski, W.; Matyjaszewski, K.; Yu, S.; Sheiko, S. S., Cylindrical Core−Shell Brushes Prepared by a Combination of ROP and ATRP. *Macromolecules* **2006,** *39* (15), 4983-4989.

107. Du, J.-Z.; Tang, L.-Y.; Song, W.-J.; Shi, Y.; Wang, J., Evaluation of Polymeric Micelles from Brush Polymer with Poly(ε-caprolactone)-b-Poly(ethylene glycol) Side Chains as Drug Carrier. *Biomacromolecules* **2009,** *10* (8), 2169-2174.

108. Neugebauer, D.; Zhang, Y.; Pakula, T.; Sheiko, S. S.; Matyjaszewski, K., Densely-Grafted and Double-Grafted PEO Brushes via ATRP. A Route to Soft Elastomers. *Macromolecules* **2003,** *36* (18), 6746-6755.

109. Qin, S.; Matyjaszewski, K.; Xu, H.; Sheiko, S. S., Synthesis and Visualization of Densely Grafted Molecular Brushes with Crystallizable Poly(octadecyl methacrylate) Block Segments. *Macromolecules* **2003,** *36* (3), 605-612.

110. Ishizu, K.; Satoh, J.; Sogabe, A., Architecture and solution properties of AB-type brush–block–brush amphiphilic copolymers via ATRP techniques. *Journal of Colloid and Interface Science* **2004,** *274* (2), 472-479.

111. Zhao, L.; Byun, M.; Rzayev, J.; Lin, Z., Polystyrene−Polylactide Bottlebrush Block Copolymer at the Air/Water Interface. *Macromolecules* **2009,** *42* (22), 9027-9033.

112. Li, X.; Prukop, S. L.; Biswal, S. L.; Verduzco, R., Surface Properties of Bottlebrush Polymer Thin Films. *Macromolecules* **2012,** *45* (17), 7118-7127.

113. Bolton, J.; Rzayev, J., Tandem RAFT-ATRP Synthesis of Polystyrene–Poly(Methyl Methacrylate) Bottlebrush Block Copolymers and Their Self-Assembly into Cylindrical Nanostructures. *ACS Macro Letters* **2012,** *1* (1), 15-18.

114. Zhang, H.; Zhang, Z.; Gnanou, Y.; Hadjichristidis, N., Well-Defined Polyethylene-Based Random, Block, and Bilayered Molecular Cobrushes. *Macromolecules* **2015,** *48* (11), 3556-3562.

115. Zhang, M.; Müller, A. H. E., Cylindrical polymer brushes. *Journal of Polymer Science Part A: Polymer Chemistry* **2005,** *43* (16), 3461-3481.

116. Bolton, J.; Rzayev, J., Synthesis and Melt Self-Assembly of PS–PMMA–PLA Triblock Bottlebrush Copolymers. *Macromolecules* **2014,** *47* (9), 2864-2874.

117. Hong, S. W.; Gu, W.; Huh, J.; Sveinbjornsson, B. R.; Jeong, G.; Grubbs, R. H.; Russell, T. P., On the Self-Assembly of Brush Block Copolymers in Thin Films. *ACS Nano* **2013,** *7* (11), 9684-9692.

118. Zehm, D.; Laschewsky, A.; Heunemann, P.; Gradzielski, M.; Prevost, S.; Liang, H.; Rabe, J. P.; Lutz, J.-F., Synthesis and self-assembly of amphiphilic semi-brush and dual brush block copolymers in solution and on surfaces. *Polymer Chemistry* **2011,** *2* (1), 137-147.

119. Lanson, D.; Schappacher, M.; Borsali, R.; Deffieux, A., Synthesis of (Poly(chloroethyl vinyl ether)-g-polystyrene)comb-b-(poly(chloropyran ethoxy vinyl ether)-g-polyisoprene)comb Copolymers and Study of Hyper-Branched Micelle Formation in Dilute Solutions. *Macromolecules* **2007,** *40* (15), 5559-5565.

120. Ariura, F.; Schappacher, M.; Borsali, R.; Deffieux, A., Janus combs with polystyrene and poly(methyl vinyl ether) branches: Design, characterization and properties. *Reactive and Functional Polymers* **2009,** *69* (7), 402-408.

121. Li, Z.; Ma, J.; Cheng, C.; Zhang, K.; Wooley, K. L., Synthesis of hetero-grafted amphiphilic diblock molecular brushes and their self-assembly in aqueous Medium. *Macromolecules* **2010,** *43* (3), 1182-1184.

122. Zehm, D.; Laschewsky, A.; Liang, H.; Rabe, J. P., Straightforward Access to Amphiphilic Dual Bottle Brushes by Combining RAFT, ATRP, and NMP Polymerization in One Sequence. *Macromolecules* **2011,** *44* (24), 9635-9641.

123. Xu, B.; Gu, G.; Feng, C.; Jiang, X.; Hu, J.; Lu, G.; Zhang, S.; Huang, X., (PAA-g-PS)-co-PPEGMEMA asymmetric polymer brushes: synthesis, self-assembly, and encapsulating capacity for both hydrophobic and hydrophilic agents. *Polymer Chemistry* **2016,** *7* (3), 613-624.

124. Gu, W.; Huh, J.; Hong, S. W.; Sveinbjornsson, B. R.; Park, C.; Grubbs, R. H.; Russell, T. P., Self-Assembly of Symmetric Brush Diblock Copolymers. *ACS Nano* **2013,** *7* (3), 2551-2558.

125. Lanson, D.; Schappacher, M.; Borsali, R.; Deffieux, A., Poly(styrene)comb-b-Poly(ethylene oxide)comb Copolymers: Synthesis and AFM Investigation of Intra- and Supramolecular Organization as Thin Deposits. *Macromolecules* **2007,** *40* (26), 9503-9509.

126. Miyake, G. M.; Weitekamp, R. A.; Piunova, V. A.; Grubbs, R. H., Synthesis of isocyanate-based brush block copolymers and their rapid self-assembly to infrared-reflecting photonic crystals. *Journal of the American Chemical Society* **2012,** *134* (34), 14249-14254.

127. Miyake, G. M.; Piunova, V. A.; Weitekamp, R. A.; Grubbs, R. H., Precisely tunable photonic crystals from rapidly self-assembling brush block copolymer blends. *Angewandte Chemie - International Edition* **2012,** *51* (45), 11246-11248.

128. Ping, J.; Qiao, Y.; Tian, H.; Shen, Z.; Fan, X.-H., Synthesis and Properties of a Coil-g-Rod Polymer Brush by Combination of ATRP and Alternating Copolymerization. *Macromolecules* **2015,** *48* (3), 592-599.

129. Jiang, Z.-Q.; Xue, Y.-X.; Chen, J.-L.; Yu, Z.-P.; Liu, N.; Yin, J.; Zhu, Y.-Y.; Wu, Z.-Q., One-Pot Synthesis of Brush Copolymers Bearing Stereoregular Helical Polyisocyanides as Side Chains through Tandem Catalysis. *Macromolecules* **2015,** *48* (1), 81-89.

130. Saito, Y.; Kikuchi, M.; Jinbo, Y.; Narumi, A.; Kawaguchi, S., Determination of the Chain Stiffness Parameter of Molecular Rod Brushes Consisting of a Polymethacrylate Main Chain and Poly(n-hexyl isocyanate) Side Chains. *Macromolecules* **2015,** *48* (24), 8971-8979.

131. Kasha, M., Energy Transfer Mechanisms and the Molecular Exciton Model for Molecular Aggregates. *Radiation Research* **1963,** *20* (1), 55-70.

132. Spano, F. C., The Spectral Signatures of Frenkel Polarons in H- and J-Aggregates. *Accounts of Chemical Research* **2010,** *43* (3), 429-439.

133. Clark, J., Intermolecular interactions in π-conjugated molecules: optical probes of chain conformation. *PhD Diss., Univ. Cambridge, Cambridge, UK* **2009**.

134. Park, S. J.; Kang, S. G.; Fryd, M.; Saven, J. G.; Park, S. J., Highly tunable photoluminescent properties of amphiphilic conjugated block copolymers. *Journal of the American Chemical Society* **2010,** *132* (29), 9931-9933.

135. Gilroy, J. B.; Lunn, D. J.; Patra, S. K.; Whittell, G. R.; Winnik, M. A.; Manners, I., Fiber-like Micelles via the Crystallization-Driven Solution Self-Assembly of Poly(3-hexylthiophene)-block-Poly(methyl methacrylate) Copolymers. *Macromolecules* **2012,** *45* (14), 5806-5815.

136. Li, J.; Li, X.; Ni, D.; Wang, J.; Tu, G.; Zhu, J., Self-assembly of poly(3-hexyl thiophene)-b-poly(ethylene oxide) into cylindrical micelles in binary solvent mixtures. *Journal of Applied Polymer Science* **2014,** *131* (23), n/a-n/a.

137. Gadt, T.; Ieong, N. S.; Cambridge, G.; Winnik, M. A.; Manners, I., Complex and hierarchical micelle architectures from diblock copolymers using living, crystallization-driven polymerizations. *Nat Mater* **2009,** *8* (2), 144-150.

138. Gwyther, J.; Gilroy, J. B.; Rupar, P. A.; Lunn, D. J.; Kynaston, E.; Patra, S. K.; Whittell, G. R.; Winnik, M. A.; Manners, I., Dimensional Control of Block Copolymer Nanofibers with a π-Conjugated Core: Crystallization-Driven Solution Self-Assembly of Amphiphilic Poly(3-hexylthiophene)-b-poly(2-vinylpyridine). *Chemistry – A European Journal* **2013,** *19* (28), 9186-9197.